

# 8

## Reggeon exchange

We have discussed analytic properties of the partial-wave amplitude  $f_{\ell}^{\pm}(t)$ . Further, having realized that moving singularities  $\ell = \alpha(t)$  in the complex angular momentum plane can be investigated also as singularities in the energy plane,  $t = t(\ell)$ , we discussed how they appear from the unphysical sheets, connected with the right (unitary) cuts of the amplitude. We found that on the first unphysical sheet partial waves can have only poles, i.e. the situation here turned out to be the same as for integer angular momenta,  $\ell = n$ .

Recall that the picture we had for integer  $n$  was dominated by poles. We put in particles (poles on the physical sheet), and they generated singularities on other sheets linked to production thresholds of two or more particles (or resonances).

It is clear that first the pole singularities must be studied. In non-relativistic quantum mechanics, by increasing the interaction strength, I can turn a resonance (a virtual state) into a real particle (a bound state). In the theory of complex angular momenta the same phenomenon takes place with the decrease of  $\ell$ : a resonance pole moves from the unphysical sheet, through the tip of the unitary cut, onto the physical sheet, see Fig. 7.4 above. In this sense  $\ell$  is akin to an interaction constant of the non-relativistic theory. So, in this lecture we are going to discuss the properties of Regge poles and the picture of the strong interactions in the pole approximation.

As we shall see later, Regge poles generate *branch cuts* in the  $\ell$  plane, in a manner similar to the generation of threshold branchings via unitarity conditions by poles (particles) in the case of integer angular momenta. The existence of these new branching singularities will seriously affect some of the results of the present lecture.

### 8.1 Properties of the Regge poles. Factorization

In the previous lecture we have introduced two analytic functions  $f_\ell^\pm(t)$ . What sort of amplitude corresponds to a single pole in the partial wave of definite signature? Substituting the pole expression

$$f_\ell^\pm(t) = \frac{r^\pm(t)}{\ell - \alpha^\pm(t)}$$

into the Sommerfeld–Watson integral (7.22) results in the following contribution to the scattering amplitude in the  $s$  channel:

$$A^\pm(s, t) = -\frac{\pi}{2} r \frac{2\alpha + 1}{\sin \pi\alpha} [P_\alpha(-z) \pm P_\alpha(z)], \quad z = 1 + \frac{2s}{t - 4\mu^2}, \quad (8.1)$$

where we have suppressed the signature label  $\pm$  for the residue,  $r = r^\pm(t)$  and the trajectory,  $\alpha = \alpha^\pm(t)$ .

Let us look at the singularities of  $A^+(s, t)$ . The amplitude with a positive signature has poles at those  $t$  values for which  $\alpha^+(t) = 2n$  is an even number. Assume, e.g. that  $\alpha(t) = 0$  at  $t = m_0^2$ . This means that if  $t \rightarrow m_0^2$ , the physical partial wave  $f_0(t)$  tends to infinity. Indeed, near the pole we have

$$f_\ell^+(t) \simeq \frac{r(t)}{\ell - \alpha(m_0^2) - \alpha'(m_0^2)(t - m_0^2)},$$

and, since  $\alpha(m_0^2) = 0$ ,

$$f_0(t) \simeq \frac{r(m_0^2)}{\alpha'(m_0^2) \cdot (m_0^2 - t)}.$$

Then the pole term of  $A^+(s, t)$ ,

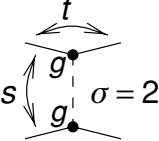
$$A_0^+(s, t) = \frac{r}{\alpha' m_0^2 - t} = s \begin{array}{c} \overbrace{\hspace{1cm}}^t \\ \swarrow \quad \searrow \\ g \bullet \quad \bullet g \\ \downarrow \quad \uparrow \\ g \bullet \quad \bullet g \\ \swarrow \quad \searrow \\ \underbrace{\hspace{1cm}}_\sigma \end{array} \sigma = 0$$

coincides with the exchange diagram for a spin  $\sigma = 0$  particle (with residue  $g^2 = r/\alpha'$ ).

The next singularity of  $A^+$  appears at some  $t = m_2^2$  where  $\alpha(m_2^2) = 2$ :

$$A_2^+(s, t) = \frac{r(m_2^2)}{\alpha'(m_2^2)} \frac{2\alpha(m_2^2) + 1}{m_2^2 - t} P_2(z).$$

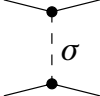
This is, however, just the contribution of the diagram for a spin  $\sigma=2$  particle exchange:



The diagram shows two vertices connected by a vertical line labeled  $\sigma = 2$ . Each vertex has two external lines. The top vertex has a line labeled  $t$  and a line labeled  $g$ . The bottom vertex has a line labeled  $g$  and a line labeled  $s$ . The diagram is equated to the mathematical expression  $= \Gamma_{\mu_1\mu_2} \frac{d_{\mu_1\mu_2,\mu_3\mu_4}}{m_\sigma^2 - t} \Gamma_{\mu_3\mu_4} = g^2 \frac{P_2(\cos \Theta_t)}{m_\sigma^2 - t}$ .

Hence, in the physical points of its proper signature,  $\alpha^+ = 2n$ , the trajectory  $\ell = \alpha^+(t)$  reproduces the particle (resonance) exchange with even spin values for the amplitude (8.1). Similarly, the contribution of the Regge pole of negative signature  $A^-(s, t)$  contains the exchange of odd spin particles.

Let us note that a trivial generalization of a Feynman diagram



The diagram shows two vertices connected by a vertical line labeled  $\sigma$ . Each vertex has two external lines. It is equated to the mathematical expression  $= g^2 \frac{P_\sigma(z)}{m_\sigma^2 - t}$ .

to the case of non-integer spin  $\sigma$ , based on the assumption that the mass is a continuous function of the spin,  $m_\sigma^2 \rightarrow m^2(\ell)$ , does not give a reggeon amplitude (8.1). Indeed, the amplitude (8.2) has a pole for any  $\ell$  value, whereas in the expression (8.1) the poles emerge in integer points only. In addition, the Regge amplitude (8.1) bears a non-trivial complexity due to the factor  $[P_\alpha(-z) \pm P_\alpha(z)]$ , which cannot be obtained by the generalization (8.2) either.

The expression (8.1) can be considered as the contribution to the scattering amplitude coming from the exchange of a ‘particle’ of variable spin – a *reggeon* – with a propagator

$$\frac{[P_{\alpha(t)}(-z) \pm P_{\alpha(t)}(z)]}{\sin \pi\alpha(t)} \quad \text{instead of the usual} \quad \frac{P_\sigma(z)}{m_\sigma^2 - t}.$$

The analogy between the reggeon and the particles (resonances) will be complete, if we find that the reggeon residue is factorizable. In this case we will be able to speak not only about ‘propagation’ of the Regge pole but also about the vertices of its ‘emission’ and ‘absorption’.

As in the case of resonances, the factorization is, essentially, a consequence of unitarity. We presented a formal proof of factorization for resonances by diagonalizing the  $S$ -matrix in Lecture 3. Let us show in a more transparent way how factorization appears. Consider, e.g. three different reactions

$$\pi\pi \rightarrow \pi\pi, \quad \pi K \rightarrow \pi K, \quad KK \rightarrow KK. \tag{8.3a}$$

For each amplitude (8.3a) its own partial waves can be introduced in the  $t$ -channel:

$$\varphi_\ell(\pi\pi \rightarrow \pi\pi), \quad g_\ell(\pi\pi \rightarrow K\bar{K}), \quad h_\ell(K\bar{K} \rightarrow K\bar{K}). \quad (8.3b)$$

In the region  $4\mu^2 < t < 16\mu^2 < 4m_K^2$  there exists only one intermediate state and the unitarity condition takes the simple form

$$\text{Im } \varphi_\ell(t) = \frac{1}{2} \left[ \text{Diagram 1} + \text{Diagram 2} \right], \quad \text{Im } \varphi_\ell(t) = C_\ell \varphi_\ell(t) \varphi_\ell^*(t); \quad (8.4a)$$

$$\text{Im } g_\ell(t) = \frac{1}{2} \left[ \text{Diagram 1} + \text{Diagram 2} \right], \quad \text{Im } g_\ell(t) = C_\ell \varphi_\ell(t) g_\ell^*(t); \quad (8.4b)$$

$$\text{Im } h_\ell(t) = \frac{1}{2} \left[ \text{Diagram 1} + \text{Diagram 2} \right], \quad \text{Im } h_\ell(t) = C_\ell g_\ell(t) g_\ell^*(t). \quad (8.4c)$$

Here  $C_\ell = \tau(t - 4\mu^2)^\ell$  with  $\tau = \omega_c/16\pi k_c$  the invariant phase-space volume (3.7) of the  $\pi\pi$  state, and the factor  $(t - 4\mu^2)^\ell$  appears owing to the definition of the partial waves  $\varphi_\ell, g_\ell, h_\ell$ , see (7.30). We have seen already that the unitarity conditions (8.4) can be continued onto arbitrary complex  $\ell$  values by rewriting them in terms of discontinuities on the cuts:

$$\frac{1}{2i} [\varphi_\ell(+)-\varphi_\ell(-)] = C_\ell \varphi_\ell(-)\varphi_\ell(+), \quad (8.5a)$$

$$\frac{1}{2i} [g_\ell(+)-g_\ell(-)] = C_\ell \varphi_\ell(-)g_\ell(+), \quad (8.5b)$$

$$\frac{1}{2i} [h_\ell(+)-h_\ell(-)] = C_\ell g_\ell(-)g_\ell(+), \quad (8.5c)$$

where  $(+) = t + i\varepsilon$ ,  $(-) = t - i\varepsilon$ . Equations (8.5) allow us to move to the first unphysical sheet and check there the singularities of the partial amplitudes (see Lecture 7):

$$\varphi_\ell(+)=\frac{\varphi_\ell(-)}{1-2iC_\ell\varphi_\ell(-)}, \tag{8.6a}$$

$$g_\ell(+)=\frac{g_\ell(-)}{1-2iC_\ell\varphi_\ell(-)}, \tag{8.6b}$$

$$h_\ell(+)=h_\ell(-)+\frac{2iC_\ell g_\ell^2(-)}{1-2iC_\ell\varphi_\ell(-)}. \tag{8.6c}$$

For a certain  $t = t(\ell)$  (or equivalently  $\ell = \alpha(t)$ ) where the  $\pi\pi$  partial wave  $\varphi(-)$  on the unphysical sheet equals  $\varphi_\ell(-) = 1/2iC_\ell$ , every partial amplitude (8.6) acquires the same pole:

$$\varphi_\ell(t) \simeq \frac{r_{\pi\pi}(t)}{\ell - \alpha(t)}; \quad g_\ell(t) \simeq \frac{r_{\pi K}(t)}{\ell - \alpha(t)}; \quad h_\ell(t) \simeq \frac{r_{KK}(t)}{\ell - \alpha(t)}.$$

It easily follows from equations (8.6) that the residues of the amplitudes in this pole satisfy the relation

$$r_{\pi\pi} \cdot r_{KK} = r_{\pi K}^2. \tag{8.7a}$$

It is just this last expression (8.7a) which verifies the factorization of the reggeon residue:

$$r_{\pi\pi} = \tilde{g}_\pi^2, \quad r_{\pi K} = \tilde{g}_\pi \tilde{g}_K, \quad r_{KK} = \tilde{g}_K^2, \tag{8.7b}$$

with  $\tilde{g}_\pi$  and  $\tilde{g}_K$  the coupling constants of the reggeon with particles.

Hence, the contribution of the Regge pole to our amplitudes is

$$\begin{aligned} A_{\pi\pi}^\pm(s, t) &= -\frac{\pi}{2}(2\alpha + 1)[\tilde{g}_\pi(t)]^2 \cdot \frac{[P_\alpha(-z_{\pi\pi}) \pm P_\alpha(z_{\pi\pi})]}{\sin(\pi\alpha)} \\ A_{\pi K}^\pm(s, t) &= -\frac{\pi}{2}(2\alpha + 1)\tilde{g}_\pi(t)\tilde{g}_K(t) \cdot \frac{[P_\alpha(-z_{\pi K}) \pm P_\alpha(z_{\pi K})]}{\sin(\pi\alpha)} \\ A_{KK}^\pm(s, t) &= -\frac{\pi}{2}(2\alpha + 1)[\tilde{g}_K(t)]^2 \cdot \frac{[P_\alpha(-z_{KK}) \pm P_\alpha(z_{KK})]}{\sin(\pi\alpha)}. \end{aligned}$$

Here  $z_{\pi\pi}$ ,  $z_{\pi K}$ , and  $z_{KK}$  are cosines of the  $t$ -channel scattering angles of the corresponding reactions. Taking into account that at large  $s$  the cosines also factorize,

$$z_{\pi\pi} \simeq \frac{s}{2|\mathbf{p}_\pi^{(t)}|^2}, \quad z_{\pi K} \simeq \frac{s}{2|\mathbf{p}_\pi^{(t)}||\mathbf{p}_K^{(t)}|}, \quad z_{KK} \simeq \frac{s}{2|\mathbf{p}_K^{(t)}|^2},$$

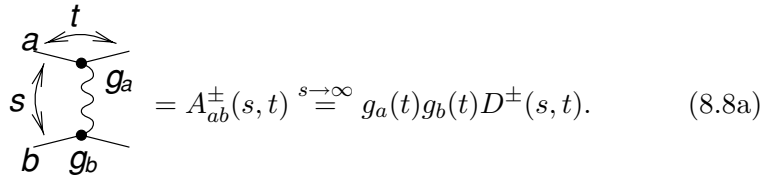
where

$$|\mathbf{p}_\pi^{(t)}| = \frac{1}{2}\sqrt{t - 4\mu^2}, \quad |\mathbf{p}_K^{(t)}| = \frac{1}{2}\sqrt{t - 4m_K^2},$$

and that

$$P_\alpha(z_{ab}) \propto z_{ab}^\alpha \sim \frac{s^\alpha}{|\mathbf{p}_a^{(t)}|^\alpha \cdot |\mathbf{p}_b^{(t)}|^\alpha},$$

we come to the main conclusion: Regge pole exchange can be described by the diagram



$$= A_{ab}^\pm(s, t) \stackrel{s \rightarrow \infty}{=} g_a(t)g_b(t)D^\pm(s, t). \quad (8.8a)$$

Here

$$D^\pm(s, t) = -\frac{(-s)^{\alpha^\pm(t)} \pm s^{\alpha^\pm(t)}}{\sin \pi\alpha^\pm(t)} = s^{\alpha^\pm(t)} \cdot \xi_\alpha^\pm \quad (8.8b)$$

is the reggeon propagator,

$$\xi_\alpha^\pm = -\frac{e^{-i\pi\alpha^\pm(t)} \pm 1}{\sin \pi\alpha^\pm(t)} \quad (8.8c)$$

is called the signature factor, and  $g_a(t)$  and  $g_b(t)$  are the vertices of the reggeon ‘emission’ and ‘absorption’.

For  $t$  values close to the mass squared of a real particle, the amplitude (8.8) transforms into the corresponding Feynman diagram. Essentially, we learned how to write the exchange for a particle whose spin depends continuously on its ‘virtual mass’.

A characteristic feature of the reggeon propagator is its complexity. The vertex functions  $g(t)$  and the trajectory  $\alpha(t)$  are real for  $t < 4\mu^2$ . The signature factor  $\xi_{\alpha(t)}$  is, however, always complex:

$$\xi_{\alpha(t)}^+ = i - \cot \frac{\pi\alpha(t)}{2}, \quad \xi_{\alpha(t)}^- = i + \tan \frac{\pi\alpha(t)}{2}. \quad (8.9)$$

Near those integer  $\ell$  values where  $\xi_\alpha$  has poles ( $\alpha^+ = 2n$ ,  $\alpha^- = 2n + 1$ ) it is almost real (as it should be for a particle exchange). For integer  $\ell$  values where  $\xi_\alpha$  has no poles ( $\alpha^+ = 2n + 1$ ,  $\alpha^- = 2n$ ), i.e. in physical points of an ‘alien’ signature,  $\xi_\alpha = i$  and the amplitude is purely imaginary (as, for example, in classical diffraction off a black target).

Hence, although the reggeon has properties of the usual particles, it differs from those essentially. Drawing a reggeon exchange, we have to understand that it corresponds to some real states in the  $s$ -channel. This means that it is not an elementary object but a complex one (an ensemble of diagrams).

What these diagrams look like, what is an  $s$ -channel image of a reggeon exchange, we will investigate in Lecture 9 in detail.

## 8.2 Quantum numbers of reggeons. The Pomeranchuk pole

In the previous section we began to draw an analogy between a reggeon and a particle, the spin of which depends on its mass continuously. However, usual particles possess also other characteristics namely, internal quantum numbers such as parity  $P$ , charge conjugation  $C$ , isotopic spin and its projection,  $I$  and  $I_3$ , strangeness  $S$ , baryon number  $B$ , etc. Do these exist for reggeons?

The answer is simple, and it is contained in the very origin of the Regge poles. We have come to Regge poles by analytically continuing the  $t$ -channel unitarity condition. This condition is, however, diagonal not only in the total angular momentum  $j$  but also with respect to arbitrary conserved quantum numbers (that commute with  $j$ ). This means that, without noticing it, in fact we have obtained a Regge trajectory from an amplitude with definite baryon charge, isospin, strangeness etc. in the  $t$ -channel. Since the unitarity conditions for amplitudes with different quantum numbers are continued independently, it is natural to expect that the corresponding trajectories  $\alpha(t)$  will also be different.

Consequently, definite quantum numbers can be assigned to every Regge trajectory. That is, unless there is a special degeneracy, either accidental or following from some symmetry. (The isotopic invariance of strong interactions may serve as an example of such a symmetry, which leads to degenerate trajectories with different electric charges but belonging to one isotopic multiplet.) For  $t > 0$  on each trajectory there are only resonances with the same quantum numbers, differing only by their spins.

Let us note that a particle situated on a Regge trajectory can be considered as a composite one, formed of two particles in the  $t$ -channel reaction. One may ask whether all particles are placed on trajectories or if there are also *non-reggeized*, elementary ones. We postpone the theoretical investigation of this question to Lecture 11. Here we just sketch the experimental situation.

Virtually all the well established resonances, both bosonic and fermionic ones (fermionic Regge poles will be considered in Section 8.7), fit the

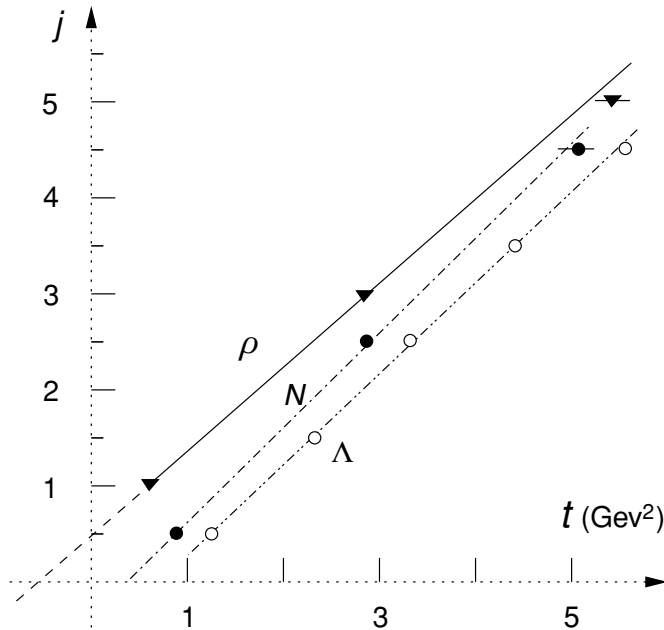
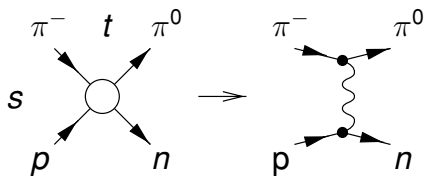


Fig. 8.1 Chew–Frautschi plots. Dot-dashed lines sample baryon trajectories  $N_{I=1/2}$  and  $\Lambda_{I=0}$ , the latter demonstrating degeneracy in signature.

Regge trajectories as demonstrated by Fig. 8.1. With a good accuracy, the trajectories turn out to be linear, having approximately equal slopes (these are the so-called Chew–Frautschi diagrams).

Extrapolating the trajectory to  $t = 0$  on Fig. 8.1, we obtain a prediction for the asymptotics of the scattering amplitude in the crossing channel. Hence, an interesting possibility appears to verify directly the theory of complex angular momenta.



As an example, let us consider the pion–nucleon charge exchange reaction  $\pi^- p \rightarrow \pi^0 n$ . At high energies  $s$  the forward amplitude ( $t = 0$ ) shows a power growth:

$$A(s, 0) \propto s^{\alpha(0)} = s^{0.57 \pm 0.02}. \tag{8.10}$$

In a system of two pions with isospin  $I = 1$  the vector and tensor resonances  $\rho_{\sigma=1}(770)$  and  $\rho_{\sigma=3}(1690)$  are well established. A straight line going through these points in Fig. 8.1 crosses the  $t=0$  axis at  $j = \alpha(0) \simeq 0.5$ , in a good agreement with (8.10).



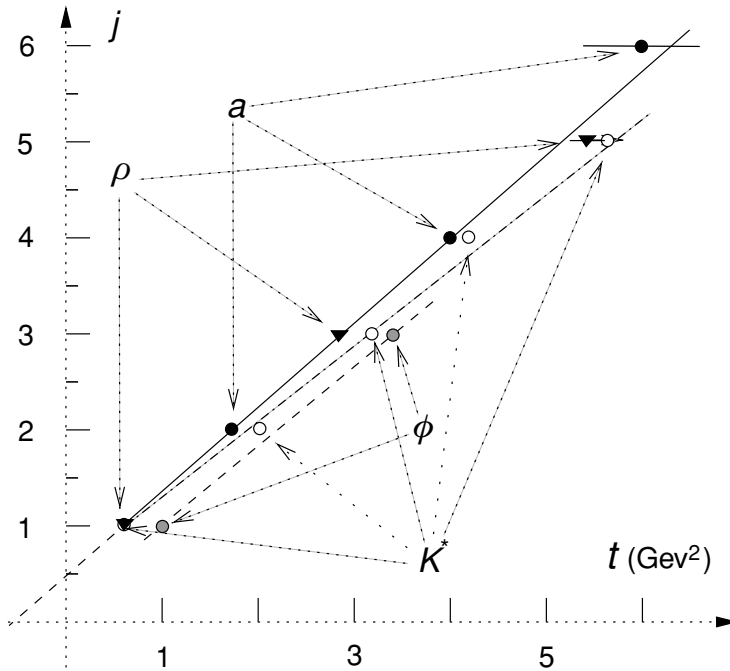
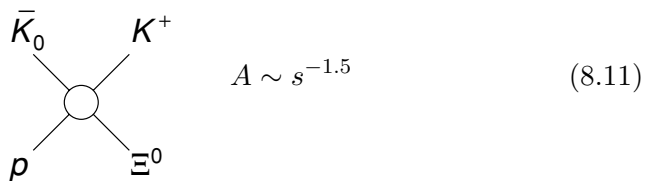


Fig. 8.2 Examples of meson Regge trajectories.

Some meson trajectories are displayed in Fig. 8.2. Series of  $\rho$  and  $a$  mesons show *signature degeneracy*. The masses of *isoscalars*  $\omega$ ,  $f$  practically coincide with the masses of their respective *isovector* partners,  $\rho$  and  $a$ , and obviously lie on the same line. Strange  $I = \frac{1}{2}$  mesons  $K^*$  with spins from 1 to 5 seem to be approximately degenerate in signature too. The situation with mass spectra of *unnatural parity* mesons, like *pseudoscalars*  $\pi$  and  $\eta$ , *axial vector* resonances, etc. is less clear.

The theory of complex angular momenta finds a striking confirmation in the so-called ‘exotic’ reactions, when the quantum numbers of the  $t$ -channel reaction are such that neither of the resonances can contribute. For example, the reaction



requires strangeness exchange  $S=2$ . Mesons with strangeness 2 were not observed. (Note that their existence would contradict the quark model.)

Correspondingly, in the experiment the amplitude (8.11) falls rapidly with energy. Even if a Regge trajectory with such quantum numbers exists, on the Chew–Frautschi diagram Fig. 8.2 it must lie much lower than the usual trajectories. This means that the corresponding resonances, if any, would have much larger masses.

Thus, we came to the conclusion that a reggeon has all quantum numbers of usual particles (except spin), and, in addition, possesses a new characteristic – the signature  $P_j = (-1)^j$ .

### 8.2.1 ‘Naturality’

We will discuss in Section 8.5 how to determine reggeon quantum numbers by considering the  $\pi N$  and  $NN$  scattering amplitudes. Here we will make only the following remark. For even-spin particles ( $\ell = \alpha^+$  trajectory) the positive parity is natural:  $J^P = 0^+, 2^+, 4^+$ , i.e. scalars and tensors. The states  $J^P = 0^-, 2^-, 4^-$ , i.e. pseudoscalars and pseudotensors, are of unnatural parity. For odd-spin particles ( $\ell = \alpha^-$  trajectory) we observe the opposite situation: the states  $J^P = 1^-, 3^-, 5^-, \dots$  (vectors, tensors) have natural parities while  $J^P = 1^+, 3^+, 5^+, \dots$  (pseudovectors, pseudotensors) unnatural ones.

To make the notion of ‘naturalness’ independent of the signature, it is convenient to introduce, instead of the usual spatial parity  $P$ , a new quantum number  $P_r$

$$P_r \equiv P \cdot P_j = P(-1)^j \quad (8.12a)$$

which characterizes the ‘pseudity’ of particles lying on a given Regge trajectory:

$$\begin{array}{ll} P_r = +1 & \left\{ \begin{array}{l} \alpha^+ : 0^+, 2^+, 4^+, \dots \\ \alpha^- : 1^-, 3^-, 5^-, \dots \end{array} \right. \\ \text{‘natural parity’} & \\ P_r = -1 & \left\{ \begin{array}{l} \alpha^+ : 0^-, 2^-, 4^-, \dots \\ \alpha^- : 1^+, 3^+, 5^+, \dots \end{array} \right. \\ \text{‘unnatural parity’} & \end{array}$$

The same procedure is carried out for the charge ( $C$ ) parity. Let me remind you that the  $C$ -parity can be introduced only if the charge conjugation of the system of particles leads to the same system (we are interested in  $t$ -channel states). For example, for the  $\pi^+\pi^-$ -pair we have  $C = (-1)^\ell$ , with  $\ell$  the orbital moment. To characterize the charge parity independently of the signature, we introduce the quantum number  $C_r$ :

$$C_r \equiv C(-1)^j, \quad (8.12b)$$

which in our case ( $j = \ell$ ) gives  $P_r = (-1)^{\ell+j} = +1$ . If so, on trajectories with ‘normal’ charge and space parities,  $P_r = C_r = +1$ , lie mesons with

$$J^{PC} : 0^{++}, 1^{--}, 2^{++}, 3^{--}, \dots$$

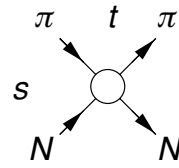
A  $t$ -channel state with a non-zero isospin,  $I \neq 0$ , does not have a definite  $C$ -parity since the charge conjugation does not commute with isospin. Then one introduces instead the  $G$ -parity which is determined via  $C$ -parity of the neutral component of the multiplet,

$$G = C(-1)^I, \quad G_r \equiv C_r(-1)^I, \tag{8.12c}$$

and analogously to (8.12b) we have a signature-independent quantum number  $G_r$ .

### 8.2.2 High energy symmetry

One of the most important consequences of the reggeized exchange is the appearance of a new symmetry (absent at low energies) in the high energy asymptotics of a two-particle amplitude. Let us demonstrate this by considering pion–nucleon scattering.



Since  $I_\pi = 1$  and  $I_N = \frac{1}{2}$ , for this process two  $t$ -channel states are possible, with isospins  $I = 0, 1$ :

$$A(s, t) = C_0 A_0^{(t)} + C_1 A_1^{(t)}, \tag{8.13a}$$

while in the  $s$ -channel there can be states with isospins  $I = \frac{1}{2}$  and  $\frac{3}{2}$ :

$$A(s, t) = C_{\frac{1}{2}} A_{\frac{1}{2}}^{(s)} + C_{\frac{3}{2}} A_{\frac{3}{2}}^{(s)}. \tag{8.13b}$$

The amplitudes  $A_0, A_1, A_{\frac{1}{2}}$  and  $A_{\frac{3}{2}}$  are not independent;  $A_{\frac{1}{2}}$  and  $A_{\frac{3}{2}}$  can be expressed in terms of  $A_0, A_1$  and vice versa.

Asymptotically  $A(s, t)$  can be determined by the contribution of the leading Regge pole. Consider, e.g. the case  $\alpha_0(t) > \alpha_1(t)$ . Then the reggeon exchange with an isospin  $I = 0$  dominates and

$$A(s, t) \stackrel{s \rightarrow \infty}{\simeq} C_0 A_0. \tag{8.14}$$

The equality (8.14) leads to a definite relation between the  $s$ -channel amplitudes  $A_{\frac{1}{2}}$  and  $A_{\frac{3}{2}}$ : both contributions are expressed in terms of  $A_0$  and have the same energy dependence. Note that there is nothing of this kind in the low-energy region. For example, in the amplitude  $A_{\frac{3}{2}}$  there is a magnificent resonance  $\Delta(1236)$ . Having isospin  $I = \frac{3}{2}$ , it is obviously

absent in  $A_{\frac{1}{2}}$ ; as a result, the energy profiles of  $A_{\frac{1}{2}}$  and  $A_{\frac{3}{2}}$  are essentially different.

Moreover, let us examine contributions of Regge poles with opposite signatures to, e.g. the  $\pi^+N \rightarrow \pi^+N$  amplitude,

$$A_{\pi^+N}(s, t) = A_{\pi^+N}^+(s, t) + A_{\pi^+N}^-(s, t). \tag{8.15a}$$

If  $A^-$  is negligible in the  $s \rightarrow \infty$  limit (which is the case as we shall see shortly), the full amplitude (8.15a) becomes  $s \leftrightarrow u$  symmetric and we obtain

$$A_{\pi^+N}(s, t) \simeq A_{\pi^-N}(s, t). \tag{8.15b}$$

It is important to stress that this statement is *stronger* than that of the Pomernanchuk theorem about the equality of total particle and antiparticle *cross sections*, since (8.15b) holds for *amplitudes*, at arbitrary  $t$ .

So, the very existence of quantum numbers for Regge poles introduces an additional symmetry that manifests itself at high energies when among all possible  $t$ -channel quantum numbers only those survive that ensure the maximal energy exponent – the leading Regge trajectory.

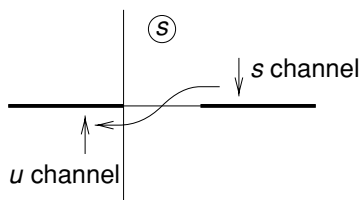
### 8.2.3 Vacuum pole

Continuing the discussion of reggeon quantum numbers, let us ask whether we could say which of the poles is the rightmost? The answer is:

in the interval  $0 \leq t \leq 4\mu^2$  (of which  $t = 0$  is the point of the most interest to us) the *rightmost pole* in the  $j$ -plane has to have positive signature,  $P_j = +1$ , and all the quantum numbers of the *vacuum*.

First we look at the signature and show that the leading pole is not allowed to have  $P_j = -1$ . Indeed, owing to the optical theorem

$$\sigma_{ab} \propto \text{Im } A_{ab}(s, t) = g_a g_b s^\alpha \cdot \text{Im } \xi_\alpha > 0.$$

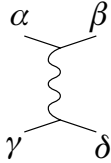


If the signature were negative, that is the amplitude was *odd* with respect to  $s \rightarrow -s$ , this would result in a *negative cross section* for the crossing  $u$ -channel reaction,  $\sigma_{\bar{a}b} \propto \text{Im } A_{\bar{a}b} \simeq \text{Im } A_{ab}(-s) < 0$ , violating the  $s$ -channel unitarity.

Physically,  $t$ -channel unitarity taught us only that the trajectories  $\alpha^+(t)$  and  $\alpha^-(t)$  were different. To acquire a more subtle information, namely  $\alpha^+(t) > \alpha^-(t)$ , we need to turn to the  $s$ -channel unitarity (which, as you remember, is a substitute for ‘potential’ for the  $t$ -channel).

Further, it is clear that the leading pole cannot have non-zero strangeness, baryon charge and alike, since in such a case the partial cross section of the corresponding non-diagonal transition would have been asymptotically larger than the total one,  $\sigma_{ab \rightarrow a'b'} > \sigma_{ab}^{\text{tot}}$ .

A bit more tricky is the situation with quantum numbers like isospin when a diagonal transition  $ab \rightarrow ab$  can still correspond to a  $I \neq 0$  state in the  $t$ -channel. We shall clarify the logic of the proof by an example for which we take  $\pi\pi$  scattering. The pion being an isovector ( $I_\pi = 1$ ), three two-pion states are possible, with  $t$ -channel isospin values  $I = 0, 1, 2$ .



These states are described, correspondingly, by the scalar product of two isovectors ( $I=0$ ), their vector product ( $I=1$ ) and the symmetric irreducible (zero trace) tensor:

$$\begin{aligned}
 A_{\alpha\beta\gamma\delta}^{(0)} &= \delta_{\alpha\beta}\delta_{\gamma\delta} \cdot A_0, \\
 A_{\alpha\beta\gamma\delta}^{(1)} &= \sum_{\sigma} \varepsilon_{\alpha\beta\sigma}\varepsilon_{\gamma\delta\sigma} \cdot A_1, \\
 A_{\alpha\beta\gamma\delta}^{(2)} &= \sum_{\rho_1, \rho_2} M_{\alpha\beta}^{\rho_1\rho_2} M_{\gamma\delta}^{\rho_1\rho_2} \cdot A_2; \quad M_{\alpha\beta}^{\rho_1\rho_2} = \delta_{\alpha}^{\rho_1}\delta_{\beta}^{\rho_2} + \delta_{\alpha}^{\rho_2}\delta_{\beta}^{\rho_1} - \frac{2}{3}\delta_{\alpha\beta}\delta^{\rho_1\rho_2}.
 \end{aligned}$$

Now we have to prove that the rightmost pole must be contained by  $A_0$ . Obviously, it cannot belong to  $A_1$ , since  $\pi\pi$  is a symmetric (Bose) system and therefore the isospin-asymmetric states, like  $I=1$ , correspond to *odd* signature.

So only  $A_2$  remains under suspicion. Let us consider a diagonal transition – an elastic zero-angle scattering process:  $\alpha = \beta, \gamma = \delta$ . Fix the charge ( $I_3$ ) of one of the  $\pi$ -mesons, say,  $\gamma = \delta = 2$  and examine one by one the total cross sections of the three isotopic states of the other one:  $\alpha = \beta = 1, 2, 3$ . If the leading pole is part of  $A_2$ , one of the cross sections turns out to be negative, since, due to the irreducibility of the tensor  $I = 2$ ,

$$\sigma_{12 \rightarrow 12} + \sigma_{22 \rightarrow 22} + \sigma_{32 \rightarrow 32} \propto \text{Tr } M = \sum_{\alpha=1}^3 M_{\alpha\alpha}^{\rho_1\rho_2} = 0.$$

This example shows what happens with any symmetry. The idea is essentially as follows. If there is some internal symmetry, the two-particle–reggeon vertex has the structure of an irreducible tensor. However, elastic amplitudes, and thus total cross sections, are given by *diagonal elements* which sum up to zero due to the irreducibility condition, and, whichever

the detailed situation, one can always find a state whose cross section will turn out to be negative.

We conclude: if there is no degeneracy, then the rightmost pole has quantum numbers of the vacuum and signature  $P_j = +1$ . This pole was named by Gell-Mann the ‘Pomeranchuk pole’ (the name later drifted to ‘pomeron’), since it satisfies the Pomeranchuk theorem automatically. To be more precise, the ‘Pomeranchuk pole’ is called the vacuum pole with an additional condition imposed, namely, that its ‘intercept’ is

$$\alpha_{\mathbf{P}}(0) = 1, \quad (8.16)$$

the condition that, due to the optical theorem, guarantees asymptotic constancy of the total interaction cross sections.

Strictly speaking, the hypothesis (8.16) does not follow from the theory. You may ask, why would we need this hypothesis in the first place? What is so attractive about asymptotically constant cross sections?

First of all, our interaction is *strong* and we see no reason why cross sections should fall with the increase of energy. But if  $\sigma_{\text{tot}}$  does not fall, then the constancy remains the only option, since any positive power would violate the Froissart theorem.

A more serious argument is the experimental situation. With the increase of the incident energy  $p_{\text{lab}} = s/2m$  by hundred times, from  $10^{10}$  to  $10^{12}$  eV where the measurements were carried out, the total proton–proton and pion–proton cross sections change only by ten percent.\* Consequently, it is natural to assume that the cross sections are basically constant, while the observed relatively small deviations are driven by correction effects that are slower than a power of  $s$  (e.g. logarithmic).

### 8.3 Properties of the Pomeranchuk pole

Thus, the asymptotic behaviour of the elastic amplitude at  $s \rightarrow \infty$  can be described by the vacuum pole (pomeron  $\mathbf{P}$ ) exchange as

$$A_{ab}(s, t) = g_a(t)g_b(t)\xi_\alpha s^{\alpha(t)}, \quad \xi_\alpha = i - \cot \frac{\pi\alpha(t)}{2}, \quad (8.17)$$

where for small values of  $t$  we can approximate the pomeron trajectory as  $\alpha(t) \simeq \alpha_{\mathbf{P}}(0) + \alpha'_{\mathbf{P}} \cdot t = 1 + \alpha'_{\mathbf{P}} \cdot t$ .

Let us discuss the characteristic features of the vacuum pole exchange.

---

\* Thirty years and three orders of magnitude in energy later, the cross sections  $\sigma_{pp} \simeq \sigma_{p\bar{p}}$  have grown by about 50%, see below Fig. 14.3, page 378. (ed.)

## 8.3.1 Pomeron theorem

The Pomeron theorem,

$$\sigma_{ab}^{\text{tot}} = \sigma_{\bar{a}\bar{b}}^{\text{tot}}, \quad (8.18)$$

is a consequence of the fact that the signature of the  $\alpha_{\mathbf{P}}(t)$  trajectory is positive. In addition,  $\text{Re } A(s, 0) = 0$ , since  $j = \alpha_{\mathbf{P}}(0) = 1$  is a point of ‘alien’ signature and the signature factor in (8.17) is purely imaginary. This means that the pomeron exchange is analogous, in the NQM language, to diffraction off absorbing target.

## 8.3.2 Factorization of total cross sections

Factorization relation for total cross sections,

$$(\sigma_{ab}^{\text{tot}})^2 = \sigma_{aa}^{\text{tot}} \cdot \sigma_{bb}^{\text{tot}}, \quad (8.19)$$

follows from the factorisation of the reggeon exchange (8.8). The knowledge of the  $\pi N$  and  $NN$  cross sections enables us to predict

$$\sigma_{\pi\pi} = \frac{(\sigma_{\pi N})^2}{\sigma_{NN}} \simeq \frac{(25 \text{ mb})^2}{40 \text{ mb}} \simeq 16 \text{ mb}.$$

Unfortunately, so far there is no experimental verification for the total cross sections. For *inelastic* cross sections such expectations have been verified and they agree reasonably well.

## 8.3.3 Factorization of differential cross sections

Consider reactions of excitation of a target hadron ( $b \rightarrow c$ ) by different projectiles ( $a$ ). For example, proton (nucleon) excitation,  $N \rightarrow N^*$ , by pion and kaon beams. Relations like

$$\frac{\sigma(\pi N \rightarrow \pi N^*)}{\sigma(KN \rightarrow KN^*)} = \frac{\sigma(\pi N \rightarrow \pi N)}{\sigma(KN \rightarrow KN)}$$

were checked many times. As it turns out, the factorization of differential cross sections at high energies generally holds within 10–20%.

## 8.3.4 Falloff of charge-exchange reactions

Another consequence of the pomeron picture is the disappearance of all sorts of ‘charge-exchange’  $2 \rightarrow 2$  reactions in the high-energy limit. Indeed, any such process corresponds to a non-diagonal transition (e.g.  $\pi^- p \rightarrow \pi^0 n$ ) with non-vacuum quantum numbers in the  $t$ -channel. Being

devoid of the vacuum-pole exchange, its amplitude must therefore be *suppressed* as a power of  $s$  relative to the elastic amplitude.

### 8.3.5 Growing radius and shrinkage of diffractive cone

Substituting the elastic scattering amplitude

$$A_{ab} = s \cdot g_a g_b e^{(\alpha_{\mathbf{P}}(t)-1) \ln s} \left( i - \cot \frac{\pi \alpha_{\mathbf{P}}(t)}{2} \right) \quad (8.20)$$

in the expression for the differential cross section, at small  $t \simeq -\mathbf{q}_{\perp}^2$  we obtain

$$\frac{d\sigma}{dq^2} = \frac{1}{16\pi} \left| \frac{A}{s} \right|^2 \simeq \frac{g_a^2 g_b^2}{16\pi} e^{-2\alpha'_{\mathbf{P}} \ln s \cdot q_{\perp}^2}. \quad (8.21a)$$

Hence, the diffractive cone *shrinks* logarithmically with the increase of  $s$ :

$$q_{\text{char}}^2 \simeq \frac{1}{2\alpha'_{\mathbf{P}} \ln s}, \quad (8.21b)$$

which corresponds to the growth of the radius of interaction

$$\rho_0 \sim \sqrt{\alpha'_{\mathbf{P}} \ln s}. \quad (8.21c)$$

### 8.3.6 Impact parameter diffusion

What is the picture in the impact parameter plane corresponding to the pomeron exchange? Let us invert the Fourier representation (5.43) for the impact parameter function  $f(\boldsymbol{\rho}, s)$ ,

$$f(\boldsymbol{\rho}, s) = \frac{\pi}{k_c^2} \int \frac{d^2 \mathbf{q}_{\perp}}{(2\pi)^2} e^{-i(\mathbf{q}_{\perp} \cdot \boldsymbol{\rho})} A(s, -q_{\perp}^2).$$

Substituting for  $A$  the pomeron amplitude (8.20) we obtain

$$\begin{aligned} f(\boldsymbol{\rho}, s) &\simeq 4\pi i g_a(0) g_b(0) \int \frac{d^2 \mathbf{q}_{\perp}}{(2\pi)^2} e^{-i(\mathbf{q}_{\perp} \cdot \boldsymbol{\rho}) - \alpha'_{\mathbf{P}} q_{\perp}^2 \ln s} \\ &= \frac{i g_a g_b}{\alpha'_{\mathbf{P}} \ln s} \exp \left( -\frac{\rho^2}{4\alpha'_{\mathbf{P}} \ln s} \right). \end{aligned} \quad (8.22)$$

We see that the partial amplitude is not *saturated*; on the contrary, its magnitude is small at large values of  $\ln s$ : the target is not at all 'black' but rather 'grey' and gets increasingly transparent with the growth of the energy. At the same time the interaction radius also grows since the exponential falloff of  $f(\boldsymbol{\rho})$  starts at larger and larger impact parameters as shown in Fig. 8.3.



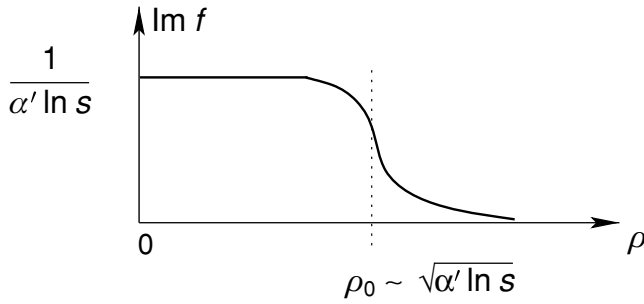


Fig. 8.3 Impact parameter profile of the partial wave corresponding to pomeron exchange.

The total cross section remains constant,

$$\int d^2\rho \operatorname{Im} f(\rho, s) = g_a g_b = \sigma^{\text{tot}} = \text{const},$$

but this is achieved in a rather peculiar way.

By the way, as we have already seen in Section 5.6, the growth of the radius  $\rho_0(s) \propto \sqrt{\ln s}$  corresponds to a ‘random walk’ of a point in which the interaction of the projectile with the target takes place in the impact parameter plane. This fact can be also seen directly from (8.22) for  $f(\rho, s)$  which very expression is nothing but the Green function of the two-dimensional diffusion process,

$$\frac{\partial}{\partial \xi} f(\rho, \xi) - \alpha' \nabla_\rho^2 f(\rho, \xi) = \delta(\rho) \delta(\xi), \tag{8.23}$$

with  $\xi = \ln s$  in the rôle of the diffusion time.

### 8.3.7 Properties of the pomeron trajectory

Let us discuss the properties of  $\alpha_{\mathbf{P}}(t)$ . In the interval  $0 \leq t \leq 4\mu^2$  we can make two statements, namely, that:

- (1) the pomeron trajectory  $\alpha_{\mathbf{P}}(t)$  is real and
- (2) monotonically increasing,  $\alpha'_{\mathbf{P}}(t) > 0$ .

Indeed, the imaginary part of the amplitude

$$\operatorname{Im} A(s, t) = r(t) s^{\alpha(t)}, \quad r(t) \equiv g_a(t) g_b(t), \tag{8.24}$$

remains real up to the first singularity at  $t = 4\mu^2$  where the partial wave expansion

$$\text{Im } A(s, t) = \sum_{\ell} (2\ell + 1) \text{Im } f_{\ell}(s) P_{\ell}(z_s), \quad z_s = 1 + \frac{2t}{s - 4\mu^2}, \quad (8.25)$$

diverges. Furthermore, we have  $\text{Im } f_{\ell} \geq 0$ , and  $P_{\ell}(z_s) > 0$ , together with all its derivatives. Therefore, differentiating (8.25) over  $t$  we have

$$\frac{d}{dt} \text{Im } A(s, t) > 0. \quad (8.26)$$

Substituting the pomeron amplitude (8.24),

$$\frac{d}{dt} \left( r(t) s^{\alpha(t)} \right) = r'(t) s^{\alpha(t)} + r \alpha'(t) \ln s \cdot s^{\alpha(t)} > 0. \quad (8.27)$$

Since  $s \rightarrow \infty$ , the main contribution comes from the last term in (8.27), resulting in  $\alpha'_{\mathbf{P}}(t) > 0$ . (If by any chance  $\alpha'_{\mathbf{P}}(t) = 0$ , then the second derivative will be positive at this point, etc.)

Is there a complexity in  $\alpha(t)$  for  $t < 0$ ?

Let us demonstrate that in spite of the partial wave  $\varphi_{\ell}(t)$  having the left cut, the trajectory remains regular at  $t \leq 0$ . Indeed, if  $\alpha(t)$  were complex, then  $\varphi_{\ell}(t)$  would have acquired at  $t = 0$  additional singularities in  $\ell$ :

$$\Delta\varphi_{\ell}(t) = \frac{\Delta r(t)}{\ell - \alpha(t)} + \frac{r(t)}{(\ell - \alpha(t))^2} \Delta\alpha(t).$$

We know, however, that moving singularities in  $\ell$  of  $\varphi_{\ell}(t)$  can come only from under the right cut<sup>†</sup> at  $t \geq 4\mu^2$ , see Lecture 3. Thus,  $\Delta r = \Delta\alpha \equiv 0$ . As a consequence,  $\alpha_{\mathbf{P}}(t)$  remains real also when  $t < 0$ .

For  $t > 4\mu^2$  the pomeron trajectory becomes complex. By explicitly solving the two-particle unitarity condition for the partial wave near the threshold,  $t \simeq 4\mu^2$ , it is straightforward to show that the trajectory moves onto the *upper* plane,  $\text{Im } \alpha_{\mathbf{P}}(t) > 0$ . Whether it stays there for arbitrary large  $t$  remains an open question. This is true in NQM but cannot be rigorously proved in the relativistic theory, although it appears the most natural hypothesis. If this is the case and if we could write the dispersion relation

$$\alpha_{\mathbf{P}}(t) = 1 + \frac{t}{\pi} \int_{4\mu^2}^{\infty} \frac{\text{Im } \alpha_{\mathbf{P}}(t')}{t'(t' - t)} dt', \quad (8.28)$$

<sup>†</sup> As we shall see below in Section 8.6, a branch-point singularity in the trajectory may appear at  $t = 0$  if *two* trajectories collide in this point.

then differentiating (8.28) over  $t$  an arbitrary number of times we would have *all derivatives* of  $\alpha_{\mathbf{P}}$  to be *positive* in the interval  $0 \leq t \leq 4\mu^2$ . Once again, this property holds in the NQM where the monotonic increase of  $\alpha(t)$  can be directly linked to the natural movement of the energy level (decrease of the binding) with the increase of the centrifugal barrier (angular momentum  $\ell$ ).

In the relativistic theory the representation (8.28) was not proved and so we cannot make a strong statement of the positivity of all derivatives. Nevertheless, using the  $t$ -channel unitarity condition we have demonstrated that at least its *first derivative* is positive. This is a remarkable example of how the cross-channel unitarity allows one to *partially* recover the NQM results, in particular the natural behaviour of the characteristic  $t$ -channel angular momentum.

### 8.3.8 Mesons on the pomeron trajectory?

Let us note, finally, that the Pomeranchuk pole with  $\alpha_{\mathbf{P}}(0) = 1$  differs essentially from the non-vacuum ones.

All other Regge trajectories (both the trajectories with non-vacuum quantum numbers and the subleading vacuum pole, the so-called  $\mathbf{P}'$  with  $\alpha_{\mathbf{P}'} \simeq 0.5$ ) appear to have the same slope,  $\alpha' \simeq 1 \text{ GeV}^{-2} \sim 1/m_N^2$ , while the slope of the pomeron trajectory turns out to be about four times smaller,

$$\alpha'_{\mathbf{P}} \simeq 0.27 \text{ GeV}^{-2} \sim 1/4m_N^2. \quad (8.29)$$

Moreover, so far it is not clear whether any resonances lie on the pomeron trajectory. Given the slope (8.29), we should expect a resonance with spin 2 and  $m_2^2 \sim 4 \text{ GeV}^2$  belonging to the pomeron trajectory. The experimental situation remains uncertain: there seem to be two to three candidates for such a tensor meson.

In the linear approximation for  $\alpha_{\mathbf{P}}(t)$ , the trajectory would cross the line  $\alpha(t) = 0$  at some negative  $t = m_0^2 < 0$  thus giving rise to a scalar meson with an *imaginary mass*! M. Gell-Mann advanced arguments in favour of *vanishing of the pomeron residue* at this point,  $g_{\alpha(m_0^2)} = g_0 = 0$ . Nowadays this problem is no longer considered acute, since as we will see later, at negative  $t$  the dominant rôle is played by  $\ell$ -plane singularities other than poles (Regge cuts).

## 8.4 Structure of the reggeon residue

### 8.4.1 Scattering of particles with spins

Up to now we have investigated the scattering of spinless particles (like pions) or, more precisely, the processes in which spins of participating

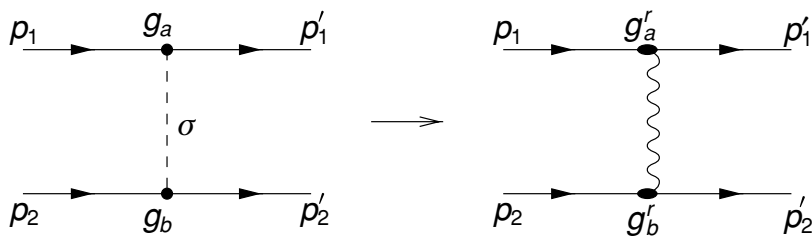


Fig. 8.4 Particle-exchange diagram (a) and the Regge-pole exchange (b).

particles were inessential. Scattering of particles with spin is an interesting problem on its own. We saw that in the spinless case a Regge amplitude differs from the amplitude of a virtual particle exchange only by the modification of the propagator ( $\sin \pi\alpha(t)$  in the denominator) and by the redefinition of the vertex  $g_a$  (Fig. 8.4). It is clear that the case of particles with spin will not differ in this respect. We could formally solve the problem by introducing particle states with definite helicity (projection of spin on the direction of three-momentum), play with spherical functions and continue the corresponding amplitudes in  $j$ . The same goal can be achieved, however, by following, essentially, the perturbation theory. We shall choose the latter path which is more rewarding.

The main problem here is how to write the *vertices*. This is easy to resolve for the case of particle exchange (Feynman graphs); a generalization to reggeons will be carried out simply by substituting the reggeon propagator for that of the exchanged particle.

The first question we have to ask is, where the *factorization* did come from? Even in the case of spinless scattering particles, the amplitude of an exchange of a particle with spin  $\sigma$  (Fig. 8.4(a)) does not factorize into a product but is given by a *sum of products*,

$$A(s, t) = \Gamma_{\{\mu_1, \dots, \mu_\sigma\}}(p_1, p'_1) D_{\{\mu\}\{\nu\}}^{[\sigma]}(q) \Gamma_{\{\nu_1, \dots, \nu_\sigma\}}(p_2, p'_2) \cdot \frac{1}{m^2 - q^2},$$

$$D_{\{\mu\}\{\nu\}}^{[\sigma]}(q) = \sum_{m=1}^{2\sigma+1} e_{\{\mu\}}^m(q) e_{\{\nu\}}^m(q),$$
(8.30)

which sum runs over all polarization states. The answer is simple: of the whole sum only one polarization survives at high energies, the one that gives the contribution with the highest power  $s$ .

Each function  $\Gamma_{\{\}} in (8.30) depends only on the momenta of particles entering the corresponding vertex and knows nothing about the large  $s$ . The momenta  $p_1$  and  $p_2$  get connected when we sum over the polarization of the exchange particle. To see how this happens, let us consider the$

example of a vector particle exchange:

$$D_{\mu\nu}^{[1]}(q) = - \sum_{m=1}^3 e_\mu^m e_\nu^m \quad \left( D_{\mu\mu}^{[1]} = 3 \right), \tag{8.31}$$

where  $\{e^m\}$  are three vectors determining a space, orthogonal to the momentum  $q$ :

$$(e^m q) = 0, \quad m = 1, 2, 3. \tag{8.32}$$

Since  $q$  is space-like, we can find two independent light-like vectors  $e^\pm$  among (8.32):

$$e^{+2} = e^{-2} = 0, \quad (e^+ e^-) = 1; \quad (e^\pm q) = 0.$$

These light-like polarization vectors can be constructed using linear combinations of the initial particle momenta,  $p_1$  and  $p_2$ . To ensure the orthogonality condition (8.32), we would have to have

$$p_1^\mu q_\mu \simeq p_2^\mu q_\mu \simeq 0. \tag{8.33}$$

Being an important characteristic feature of high-energy processes, let us check this fact in detail.

*Sudakov kinematics of high-energy 2 → 2 processes.* Before going into calculations, a simple observation first. When two particles scatter elastically, in their cms the energy is not transferred,  $q_0 = 0$ , and  $-t = \mathbf{q}^2 = 2p_c^2(1 - \cos \Theta_s) \simeq p_c^2 \cdot \Theta_s^2$ . So, for large collision energies,  $s \simeq 4p_c^2 \gg |t|$ , the scattering angle is small,  $\Theta_s \sim \sqrt{-t/s} \ll 1$ . This makes the *longitudinal* component of the momentum transfer,  $q_{||} \sim \frac{1}{2}p_c \Theta_s^2$ , much smaller than the transverse one,  $q_\perp \propto p_c \Theta_s$ ; in other words,  $\mathbf{q}$  is approximately orthogonal to the common direction of the colliding particles,  $\mathbf{z}$ . In Lorentz invariant terms, this statement is equivalent to (8.33) that we are about to verify formally.

Let us consider the kinematics of the  $2 \rightarrow 2$  scattering process in the most general case,  $p_1, p_2 \rightarrow p'_1 p'_2$ , using the Sudakov decomposition.

$$p_1 = p^+ + \gamma_1 p^-, \quad p_2 = p^- + \gamma_2 p^+; \tag{8.34a}$$

$$\gamma_{1,2} = \frac{m_{1,2}}{s} \tag{8.34b}$$

(where we have approximated  $2p^+ p^- \simeq s$ ). In the linear approximation in  $\gamma_i = \mathcal{O}(1/s)$ , the inverse relations read

$$p^+ \simeq p_1 - \gamma_1 p_2, \quad p^- \simeq p_2 - \gamma_2 p_1;$$

actually, for our purposes it often suffices to equate

$$p^+ \simeq p_1, \quad p^- \simeq p_2,$$

which approximation holds, component by component, when both  $p_0^+$  and  $p_0^-$  are large (which is true for virtually all reference frames but the laboratory frame where one of the incoming particles is at rest).

We write the transferred four-momentum as

$$q_\mu = \alpha p_\mu^+ + \beta_q p_\mu^- + q_{\perp\mu}; \quad -(q_{\perp\mu})^2 = \mathbf{q}_\perp^2 \geq 0, \quad (8.35a)$$

$$q^2 = \alpha_q \beta_q s - \mathbf{q}_\perp^2, \quad (8.35b)$$

where  $q_\perp^\mu$  lies in the  $(\mathbf{x}, \mathbf{y})$  plane.

Making use of (8.34) and (8.35) we evaluate square momenta of the outgoing particles,

$$(p'_1)^2 = (p_1 + q)^2 = (1 + \alpha_q)(\gamma_1 + \beta_q)s - \mathbf{q}_\perp^2 = m_1'^2,$$

$$(p'_2)^2 = (p_2 + q)^2 = (\gamma_2 - \alpha_q)(1 - \beta_q)s - \mathbf{q}_\perp^2 = m_2'^2,$$

to obtain

$$-\alpha_q s - \beta_q m_2^2 = m_2'^2 - m_2^2 - q^2, \quad (8.36a)$$

$$\beta_q s + \alpha_q m_1^2 = m_1'^2 - m_1^2 - q^2. \quad (8.36b)$$

In the high energy limit,  $|q^2| \sim m^2 \ll s$ , we have  $-\alpha_q \sim \beta_q \sim m^2/s \ll 1$  and (8.36) simplifies

$$-\alpha_q s \simeq m_2'^2 - m_2^2 - q^2; \quad (8.37a)$$

$$\beta_q s \simeq m_1'^2 - m_1^2 - q^2. \quad (8.37b)$$

We conclude that the 'longitudinal' contribution to the invariant  $t$  becomes negligible,

$$q^2 = q_\parallel^2 - \mathbf{q}_\perp^2, \quad q_\parallel^2 \equiv -\alpha_q \beta_q s \sim \frac{q^4}{s} \ll |q^2|,$$

so that the momentum transfer becomes essentially *transversal*,

$$q^2 = -\mathbf{q}_\perp^2 \cdot \left( 1 + \mathcal{O}\left(\frac{m^2}{s}\right) \right). \quad (8.38)$$

This statement can be enforced and applied to all components of the four-vector,

$$q_\mu = \alpha_q s \cdot \frac{p_\mu^+}{s} + \beta_q s \cdot \frac{p_\mu^-}{s} + q_{\perp\mu} \simeq q_{\perp\mu},$$

once again, in any but the laboratory frame of reference (where one of the normalized momentum vectors  $p^\pm/s$  is of the order of unity).

*Polarization vectors.* We return to the construction of the polarization vectors. Now that we have verified the condition (8.33) of the approximate orthogonality of the momentum transfer  $q$  to the  $(p_1, p_2)$  plane, we can treat  $q_\mu$  as having, say, only a  $y$  component:  $q_\mu = (q_0; q_x, q_y, q_z) \simeq (0; 0, \sqrt{-q^2}, 0)$ .

In the cms of the  $t$ -channel where  $q_\mu = (\sqrt{q^2}; \mathbf{0})$ , the polarization vectors are all space-like:

$$\begin{pmatrix} t \\ x \\ y \\ z \end{pmatrix} : \quad e^1_{(t)} = \begin{pmatrix} 0 \\ 0 \\ 0 \\ 1 \end{pmatrix}, \quad e^2_{(t)} = \begin{pmatrix} 0 \\ 0 \\ 1 \\ 0 \end{pmatrix}, \quad e^3_{(t)} = \begin{pmatrix} 0 \\ 1 \\ 0 \\ 0 \end{pmatrix}. \quad (8.39)$$

The complex Lorentz boost that takes us to the  $s$ -channel, transforms the momentum transfer as follows

$$q^\mu_{(t)} = \begin{pmatrix} -i\sqrt{-q^2} \\ 0 \\ 0 \\ 0 \end{pmatrix} \implies q^\mu = \begin{pmatrix} 0 \\ 0 \\ \sqrt{-q^2} \\ 0 \end{pmatrix};$$

it swaps the time- and  $y$ -components of a four-vector,  $t \rightarrow iy, y \rightarrow it$ , while leaving the  $x$  and  $z$  components unchanged. Under this transformation, the complex linear combinations of the first two polarizations in (8.39), in the  $s$ -channel turn into two light-like vectors:

$$e^+ = \frac{e^1 - ie^2}{\sqrt{2}} = \frac{1}{\sqrt{2}} \begin{pmatrix} 1 \\ 0 \\ 0 \\ 1 \end{pmatrix}, \quad e^- = -\frac{e^1 + ie^2}{\sqrt{2}} = \frac{1}{\sqrt{2}} \begin{pmatrix} 1 \\ 0 \\ 0 \\ -1 \end{pmatrix}. \quad (8.40)$$

From the  $t$ -channel point of view, the combinations  $e^1 \pm ie^2$  correspond to *circular polarizations* describing states with a spin projection  $\pm 1$  onto the  $\mathbf{x}$ -axis, i.e. in our case, onto the normal to the scattering plane. The light-like vectors (8.40) are nothing but the Sudakov vectors we have introduced above to represent the  $(t, z)$  interaction plane:

$$e^\pm \equiv \sqrt{\frac{2}{s}} p^\pm; \quad e^+ \simeq \sqrt{\frac{2}{s}} p_1, \quad e^- \simeq \sqrt{\frac{2}{s}} p_2. \quad (8.41a)$$

In terms of these vectors the sum over polarizations (8.31) takes the form

$$-\sum_{m=1}^3 e_\mu^m e_\nu^m = e_\mu^+ e_\nu^- + e_\mu^- e_\nu^+ - e_\mu^\perp e_\nu^\perp, \tag{8.41b}$$

where  $e^\perp = e^3 = e^3_{(t)}$  of (8.39) is a space-like unit vector normal to the scattering plane ( $\mathbf{x}$ ).

We have thus introduced convenient basis vectors. Let us see the contributions of various polarizations to the scattering amplitude:

$$= \Gamma_\mu^a(1) \cdot D_{\mu\nu}^{[1]} \cdot \Gamma_\nu^b(2) \times \frac{1}{m^2 - q^2}$$

$$\propto (\Gamma^a e^+)(e^- \Gamma^b) + (\Gamma^a e^-)(e^+ \Gamma^b) - (\Gamma^a e^\perp)(e^\perp \Gamma^b).$$

(8.42)

Which polarization leads to the leading contribution  $s^\sigma = s$  in (8.42)? The general form of the vertex for a scalar particle is

$$\Gamma_\mu^a(1) = \Gamma_\mu^a(p_1, q) = a(q^2)p_{1\mu} + b(q^2)q_\mu. \tag{8.43}$$

The term  $q_\mu$  can be dropped, see (8.32); the transverse polarization does not contribute,  $e^\perp p_1 = e^\perp p_2 = 0$ . We have

$$e_\mu^+ p_1^\mu = \frac{m_1^2}{\sqrt{2s}}, \quad e_\mu^- p_2^\mu = \frac{m_2^2}{\sqrt{2s}};$$

$$e_\mu^- p_1^\mu = \sqrt{\frac{s}{2}}, \quad e_\mu^+ p_2^\mu = \sqrt{\frac{s}{2}}.$$

Consequently, at  $s \rightarrow \infty$  of the whole sum (8.42) only one term survives,

$$\left( \Gamma_\mu^a(1) e_\mu^- \right) \left( \Gamma_\nu^b(2) e_\nu^+ \right) \sim (\sqrt{s})^2 = s,$$

in which each vertex is multiplied by the polarization vector directed along the momentum  $p_i$  of the *opposite* vertex. Hence, we can factorize the asymptotic amplitude as follows:

$$A(s, t) = \left( \Gamma_\mu^a(1) \frac{e_\mu^-}{\sqrt{s}} \right) \left( \Gamma_\nu^b(2) \frac{e_\nu^+}{\sqrt{s}} \right) \cdot s \cdot D(q^2). \tag{8.44}$$



The analogue of the reggeon residue,

$$\left( \Gamma_{\mu}^a(1) \frac{e_{\mu}^{-}}{\sqrt{s}} \right) \sim \left( \Gamma_{\mu}^a(1) \frac{p_{2\mu}}{s} \right) \equiv g_a^r(1),$$

is an invariant; in the case of spinless particles it can depend only on  $q^2$  via  $a(q^2)$ , see (8.43). If the colliding particles have non-zero spins, the vertex function  $\Gamma_{\mu}^a$  changes: it will depend also on the polarizations of the incoming and outgoing particles (1), (1'):

$$\Gamma_{\mu}^a(1) = \Gamma_{\mu}^a \left( p_1, q; \epsilon_i^{\lambda}, \epsilon_f^{\rho} \right).$$

However, the general structure of the Regge residue remains unchanged; a large contribution will still be coming only from multiplication of the vertex (1) by the polarization  $e^{-} \propto p_2$ . The residue  $g_a^r$  though will now depend not only on  $q^2$ , but also on the spin projections of the initial and final particles in the upper vertex (1) on the momentum direction of the particle (2). Thus for  $\sigma = 1$  we have obtained

$$g_a^r(1) \equiv \left( \Gamma_{\mu}^a(1) \frac{p_{2\mu}}{s} \right), \quad g_b^r(2) \equiv \left( \Gamma_{\mu}^b(2) \frac{p_{1\mu}}{s} \right). \tag{8.45}$$

Let us see now, what the residue for a  $\sigma = 2$  particle exchange looks like. A spin  $\sigma = 2$  wave function can be constructed as a symmetric product of two vector states,

$$e_{\mu_1\mu_2}^{\lambda} = e_{\mu_1}^{\lambda_1} e_{\mu_2}^{\lambda_2} + e_{\mu_2}^{\lambda_1} e_{\mu_1}^{\lambda_2}. \tag{8.46}$$

Now each vertex bears two vector indices and the amplitude has the structure

$$A(s, t) \propto \Gamma_{\mu_1\mu_2}^a(1) D_{\mu_1\mu_2, \nu_1\nu_2}^{[2]} \Gamma_{\nu_1\nu_2}^b(2) \times \frac{1}{m^2 - q^2}$$

$$D_{\mu_1\mu_2, \nu_1\nu_2} = \sum_{\lambda} e_{\mu_1\mu_2}^{\lambda} e_{\nu_1\nu_2}^{\lambda}. \tag{8.47}$$

Strictly speaking, we have to subtract from (8.46) an admixture of a  $\sigma = 0$  state to make our symmetric tensor traceless. We, however, can ignore this fact since the corresponding subtraction term contains  $g_{\mu_1\mu_2}$  which, acting on one vertex, yields no large  $s$ -dependent contribution.

Expressing (8.46) in terms of the polarizations  $e^{\pm}$ , the propagator  $D_{\mu_1\mu_2, \nu_1\nu_2}$  in (8.47) will contain various products

$$e_{\mu_1}^{+} e_{\mu_2}^{+} e_{\nu_1}^{-} e_{\nu_2}^{-}, \quad e_{\mu_1}^{+} e_{\mu_2}^{-} e_{\nu_1}^{-} e_{\nu_2}^{+}, \dots$$

It is easy to see that similarly to the case of  $\sigma = 1$ , only the term  $e_{\mu_1}^{-} e_{\mu_2}^{-} e_{\nu_1}^{+} e_{\nu_2}^{+}$  produces a contribution  $\sim s^2$ . (By the way, this term is, on

its own, a symmetric irreducible tensor since  $(e^-)^2 = 0$ .) So, the upper vertex produces

$$\left( \Gamma_{\mu_1 \mu_2}^a(1) \cdot \frac{e_{\mu_1}^-}{s} \frac{e_{\mu_2}^-}{s} \right),$$

and the analogue of the Regge residue for a spin-2 particle exchange acquires the form

$$g_a^r(1) \equiv \left( \Gamma_{\mu_1 \mu_2}^a(1) \frac{p_{2\mu_1} p_{2\mu_2}}{s^2} \right), \quad g_b^r(2) \equiv \left( \Gamma_{\nu_1 \nu_2}^b(2) \frac{p_{1\nu_1} p_{1\nu_2}}{s^2} \right). \quad (8.48)$$

How do (8.45) and (8.48) generalize to the case of non-integer angular momentum exchange? For particle exchange with an integer spin  $\sigma$  the residues  $g_a^r(1)$  turned out to be polynomials of  $p_2/s$  of the order  $\sigma$ . In the general case (which corresponds to a sum of various  $t$ -channel exchanges) the  $s$ -dependence of the amplitude becomes more complicated:

$$A(s, t) = \Gamma_a \left( p_1, q; \epsilon_i^{\lambda_1}, \epsilon_f^{\rho_1}; \frac{p_2}{s} \right) \Gamma_b \left( p_2, q; \epsilon_i^{\lambda_2}, \epsilon_f^{\rho_2}; \frac{p_1}{s} \right) \cdot s^\alpha \cdot \xi_\alpha. \quad (8.49)$$

However, the structure of the residues resembles that of simple particle exchange: each vertex depends on its internal variables (momenta and polarizations) *and* on the direction of the momentum in the opposite vertex.

In other words, the Regge factorization *remembers* the reaction plane  $(p_1, p_2)$  via the polarization vectors  $e^\pm$  which ensure the maximal contribution to the scattering amplitude.

#### 8.4.2 Quasi-elastic processes

Up to now we have been discussing  $2 \rightarrow 2$  scattering processes. Do Regge poles contribute to multi-particle production? It is easy to imagine a high-energy collision in which, say, one of the incident particles becomes excited and subsequently decays giving rise to a three-particle final state. A question can be raised, for example, for which lifetimes of the intermediate state in Fig. 8.5(a) our previous analysis will remain valid. It is possible to rigorously deduce contribution of Regge poles to such processes from the corresponding unitarity conditions for multi-particle amplitudes of the type shown in Fig. 8.5(b). I will not do that but suggest you guess the answer by looking at the diagrams describing the  $t$ -channel exchange of a particle with spin instead.

Recall the result of our analysis of reggeon amplitudes for the scattering of particles with spin: the reggeon vertex  $\Gamma$  acquired an additional dependence on the polarizations of participating particles. Similarly, here the vertex describing the  $1 \rightarrow 2$  particle conversion of Fig. 8.5(b) will depend

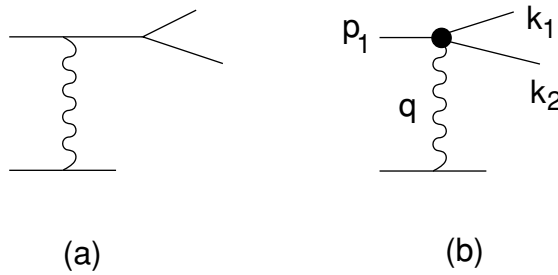


Fig. 8.5 Production of an unstable particle (a) and new reggeon vertex (b).

not only on the total momentum transfer,  $q = k_1 + k_2 - p_1$ , but also on the relative momentum  $k_1 - k_2$ ; in other words, on the two final particle momenta separately,

$$\Gamma(1) = \Gamma\left(p_1, k_1, k_2; \frac{p_2}{s}\right). \quad (8.50)$$

It is clear that some condition must be imposed on the final state momenta in order to preserve the dominance of one polarization as before: if ‘wrong’ polarizations multiplying momenta  $k_1, k_2$  produced large contributions, the factorization would be lost. First of all, we have to have, as always, the momentum transfer  $q^2$  to be finite; otherwise the very reggeon approach would fail. But this is not enough. We need not only the *total* momentum  $k_1 + k_2$  (which determines  $q^2$ ) but also *each*  $k_i$  to be ‘almost parallel’ to the incoming  $p_1$ . The final particles must *fly together*, in a dense ‘bunch’.

To give a precise meaning to ‘flying together’ let us consider a more general case of a quasi-elastic process when both incident particles produce bunches of particles which move close to the directions of the incoming hadrons as shown in Fig. 8.6. A process of this kind is called diffractive dissociation. If the relative energies of the particles in such a bunch are

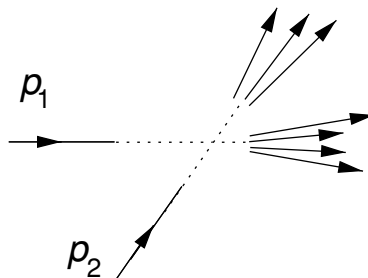


Fig. 8.6 Quasi-elastic process of (double) diffractive dissociation.

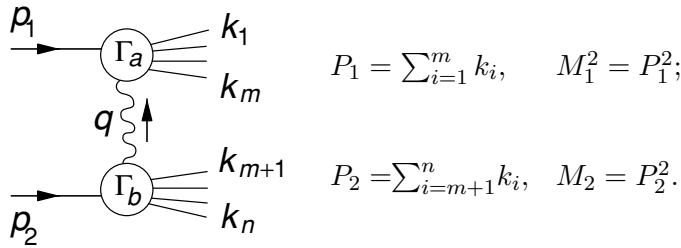


Fig. 8.7 Kinematics of high-energy diffractive dissociation.

small, it may be treated as a composite particle, and at large  $s$  the process can be effectively described as a two-particle scattering.

Let us express all momenta in terms of the Sudakov variables:

$$\begin{aligned}
 k_i &= \alpha_i p^+ + \beta_i p^- + k_{i\perp}, & q &= \alpha_q p^+ + \beta_q p^- + q_{\perp}; & (8.51) \\
 p_1 &= p^+ + \gamma_1 p^-, & p_2 &= p^- + \gamma_2 p^+.
 \end{aligned}$$

Recall that  $p^{\pm}$  are zero-norm vectors ( $p^{\pm 2} = 0, 2p^+p^- = s$ ), and  $\gamma_{1,2} \simeq m_{1,2}^2/s$ . In a frame where both scattering particles are fast (e.g. the cms of  $s$ -channel),  $p^+$  almost coincides with  $p_1$ , as  $p^-$  does with  $p_2$ . Then, in (8.51),  $-\alpha_q$  is the fraction of the momentum  $p_1$ , transferred by the reggeon to the lower vertex  $\Gamma_b$ , while  $\beta_q$  is the fraction of  $p_2$  transferred up to  $\Gamma_a$ , see Fig. 8.7. How large are the longitudinal Sudakov components of the momentum transfer  $q$ ? We have calculated them above in (8.37):

$$-\alpha_q = \frac{\Delta M_2^2 + \mathbf{q}_{\perp}^2}{s}, \quad \beta_q = \frac{\Delta M_1^2 + \mathbf{q}_{\perp}^2}{s}, \quad (8.52)$$

where  $\Delta M_1^2 = (\sum_{i=1}^m k_i)^2 - m_1^2$  and  $\Delta M_2^2 = (\sum_{i=m+1}^n k_i)^2 - m_2^2$  are the ‘excitation energies’ of the upper and lower bunches of particles.

If we keep invariant masses of the bunches *finite* in the high-energy limit,

$$M_1^2, M_2^2 = \mathcal{O}(m^2), \quad s \rightarrow \infty, \quad (8.53)$$

our previous logic remains intact and we arrive at a reggeon exchange amplitude describing the diagram of Fig. 8.7,

$$\begin{aligned}
 &A_{\alpha}(s, q^2; s_{ij}, t_{1i}, t_{2i}) & (8.54) \\
 &= \Gamma_a \left( p_1, \epsilon_1; \{k_i, \epsilon_i\}_1^m; \frac{p_2}{s} \right) \Gamma_b \left( p_2, \epsilon_2; \{k_i, \epsilon_i\}_{m+1}^n; \frac{p_1}{s} \right) s^{\alpha} \xi_{\alpha},
 \end{aligned}$$

where  $s_{ij} = (k_i + k_j)^2, t_{1i} = (p_1 - k_i)^2, t_{2i} = (p_2 - k_i)^2$ . This is just the answer that one derives as a result of a rather cumbersome procedure of analytic continuation of partial waves for multi-particle amplitudes.

The expression (8.54) is, essentially, the same as we have written for non-zero spin particle scattering. It differs from (8.49) only by the structure of the vertex functions: now  $\Gamma$  includes also the variables  $\{k_i, \epsilon_i\}$  (momenta and polarizations of the offspring) describing ‘internal movement’ of the particles in each ‘bunch’.

Under the condition (8.53), the longitudinal momentum transfer is vanishingly small at large  $s$  (in any reference frame where colliding particles are fast). For example, in the  $s$ -channel cms,  $p^\pm = \frac{1}{2}\sqrt{s}(1; 0, 0, \pm 1)$ ,

$$\begin{aligned}
 q_{||} &\equiv \alpha_q p^+ + \beta_q p^- = \frac{\sqrt{s}}{2}(\alpha_q + \beta_q, 0, 0, \alpha_q - \beta_q) \\
 &= \frac{1}{\sqrt{s}} \left( \frac{\Delta M_1^2 - \Delta M_2^2}{2}; 0, 0, -\frac{\Delta M_1^2 + \Delta M_2^2}{2} - \mathbf{q}_\perp^2 \right). \quad (8.55a)
 \end{aligned}$$

As for its contribution to the squared momentum transfer,  $q^2 = q_{||}^2 - \mathbf{q}_\perp^2$ ,

$$|q_{||}^2| = -\alpha_q \beta_q s \simeq \frac{\Delta M_1^2 \cdot \Delta M_2^2}{s} \ll \mathbf{q}_\perp^2 \simeq -q^2. \quad (8.55b)$$

Finally, let us address the question of the applicability of the reggeon inelastic diffraction amplitude (8.54), which we have vaguely formulated above as ‘to fly together’ for particles in the two bunches.

Momentum conservation in the upper and lower blocks gives us

$$-\alpha_q = 1 - \sum_{i=1}^m \alpha_i, \quad \beta_q = \sum_{i=1}^m \beta_i - \gamma_1; \quad (8.56a)$$

$$-\alpha_q = \sum_{i=m+1}^n \alpha_i - \gamma_2, \quad \beta_q = 1 - \sum_{i=m+1}^n \beta_i; \quad (8.56b)$$

in addition to

$$\mathbf{q}_\perp = \sum_{i=1}^m \mathbf{k}_{i\perp} = - \sum_{i=m+1}^n \mathbf{k}_{i\perp}.$$

To reconcile (8.56) with the condition  $-\alpha_q \sim \beta_q = \mathcal{O}(s^{-1})$  following from (8.52) and (8.53), particles in the upper bunch must have  $\alpha_i = \mathcal{O}(1)$  and small  $\beta_i$  components, and those in the lower bunch, on the contrary,  $\beta_j = \mathcal{O}(1)$  and  $\alpha_j = \mathcal{O}(s^{-1})$ . Making use of the on-mass-shell relations for the produced particles,

$$k_i^2 = \alpha_i \beta_i s - k_{i\perp}^2 = m_i^2 \quad (\alpha_i > 0, \beta_i > 0),$$

the requirements on particle momenta in the two beams read

$$\alpha_i \sim 1, \quad \beta_i = \frac{m_i^2 + \mathbf{k}_{i\perp}^2}{\alpha_i s} \ll 1, \quad i = 1 \div m; \quad (8.57a)$$

$$\beta_i \sim 1, \quad \alpha_i = \frac{m_i^2 + \mathbf{k}_{i\perp}^2}{\beta_i s} \ll 1, \quad i = (m + 1) \div n. \quad (8.57b)$$

The conditions (8.57) are just expressions of the fact that the particles fly in ‘bunches’ in both beams. For particles belonging to one beam, e.g. the upper one, we have

$$\begin{aligned} s_{ij}^{aa} &= (\alpha_i + \alpha_j)(\beta_i + \beta_j)s - (\mathbf{k}_{i\perp} + \mathbf{k}_{j\perp})^2 \\ &\sim (\alpha_i^a \beta_j^a + \beta_i^a \alpha_j^a) s \sim \left(1 \cdot \frac{m^2}{s} + \frac{m^2}{s} \cdot 1\right) s = \mathcal{O}(m^2), \end{aligned} \quad (8.58a)$$

while for particles from different beams,

$$s_{ij}^{ab} \sim (\alpha_i^a \beta_j^b + \beta_i^b \alpha_j^a) s \sim \left(1 \cdot 1 + \frac{m^2}{s} \cdot \frac{m^2}{s}\right) s = \mathcal{O}(s). \quad (8.58b)$$

In the kinematical configuration described by (8.57), the first term in (8.58b) for the invariant energy between the two particles from opposite beams is *much larger* than the second one. In fact, this is the *necessary condition* for the validity of the reggeon expression (8.54) we are looking for. It becomes clear if we rewrite the r.h.s. of (8.58b) in the following terms,

$$\alpha_i^a \beta_j^b s = 2(k_i^a \cdot e^-)(e^+ \cdot k_j^b); \quad \beta_i^a \alpha_j^b s = 2(k_i^a \cdot e^+)(e^- \cdot k_j^b).$$

We immediately see that the strong inequality

$$\alpha_i^a \beta_j^b \gg \beta_i^a \alpha_j^b \implies \left(\frac{\alpha_i}{\beta_i}\right)_{\text{bunch } a} \gg \left(\frac{\alpha_j}{\beta_j}\right)_{\text{bunch } b} \implies \frac{(\alpha_i)_a}{(\alpha_j)_b} \gg 1$$

guarantees the dominance of that one polarization that gives rise to the factorized reggeon amplitude.

At the same time, for two particles from *the same bunch* the ratio of the Sudakov variables is not too large. Indeed, if we take two particles having relatively small energy in their cms,  $\mathbf{p}_1 + \mathbf{p}_2 = 0$ ;  $p_{10}, p_{20} = \mathcal{O}(m)$ ,

$$s_{12} = (p_1 + p_2)^2 \sim 4m^2.$$

Then in the reference frame where both particles have large velocity along the  $\mathbf{z}$ -axis we have

$$p_{10} \simeq p_{1z} + \frac{m^2 + \mathbf{p}_{1\perp}^2}{2p_{10}}, \quad p_{20} \simeq p_{2z} + \frac{m^2 + \mathbf{p}_{2\perp}^2}{2p_{20}},$$

and the invariant energy reads

$$s_{12} \simeq 2(p_{10}p_{20} - p_{1z}p_{2z}) \simeq (m^2 + \mathbf{p}_{1\perp}^2) \frac{p_{20}}{p_{10}} + (m^2 + \mathbf{p}_{2\perp}^2) \frac{p_{10}}{p_{20}}$$

$$\sim m_{\perp}^2 \left( \frac{p_{20}}{p_{10}} + \frac{p_{10}}{p_{20}} \right).$$

Comparing the two expressions for  $s_{12}$  we conclude that to ‘fly together’ means for fast particles that the *ratio* of their energies is neither too small nor too large:

$$\frac{p_{20}}{p_{10}} \sim \frac{p_{10}}{p_{20}} \sim 1.$$

Meantime the *difference* of energies may be very large.

### 8.5 Elastic scatterings of $\pi$ and $N$ off the nucleon

Now we will illustrate the results of the previous section by studying the pion–nucleon and nucleon–nucleon reactions,  $\pi N \rightarrow \pi N$  and  $NN \rightarrow NN$ . To understand what Regge poles can contribute to the asymptotics of these processes at all, we have to consider first in detail the  $\pi\pi$  and  $NN$  vertices in Fig. 8.8(a).

#### 8.5.1 The pion vertex

Of all invariants that one can construct from the three four-vectors entering the pion vertex,  $\Gamma_{\pi}(p_1, q; p_2/s)$ , only one variable,  $q^2$ , survives at  $s \rightarrow \infty$ , so we have

$$g_{\pi} = \Gamma_{\pi} \left( p_1, q; \frac{p_2}{s} \right) = g_{\pi}(q^2).$$

Let us clarify which reggeon quantum numbers can be emitted in the  $\pi\pi$  vertex. To do that we have to look at the system of two pions from the

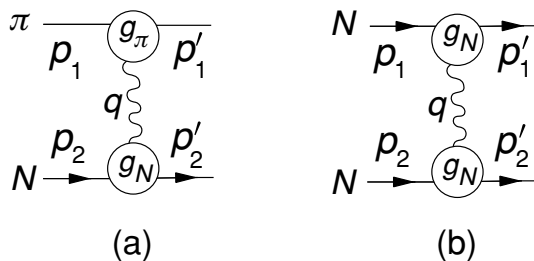


Fig. 8.8 Reggeon exchange amplitudes for  $\pi N$  (a) and  $NN$  scattering (b).

Table 8.1 *Reggeons coupled to pion → pion. All have  $P_r = C_r = +1$ .*

$I$	$G_r$	sgn	Reggeon	$\alpha(0)$	$\alpha'$	Resonance
0	+	+	<b>P</b>	1	0.25	?
			f ( <b>P'</b> )	0.5	1	$f_2(1270), f_4(2050), f_6(2510)$
1	-	-	$\rho$	0.5	1	$\rho(770), \rho_3(1690), \rho_5(2350)$
2	+	+	?			none

$t$ -channel. Since the pions are spinless, the spatial parity is

$$P = (-1)^\ell = (-1)^j \implies P_r = +1.$$

The pions are identical Bose-particles, therefore the vertex must be symmetric under the transmutation of two particles, that is of their positions and isotopic indices:  $+1 = (-1)^\ell(-1)^I = (-1)^j(-1)^I$ . Consequently,  $\pi\pi$  states with a total isospin  $I = 0, 2$  in the  $t$ -channel are linked to reggeons with positive signature and those with  $I = 1$  to ones with negative signature. The  $\pi\pi$  charge parity is also unique:  $C = (-1)^\ell \implies C_r = +1$ .

Possible quantum numbers of the  $\pi\pi$  system are listed in Table 8.1.

### 8.5.2 The nucleon vertex

Now we turn to the lower vertex in Fig. 8.8(a), that for the nucleon. In the construction of the nucleon vertex,  $\Gamma_N$ , we may employ Lorentz invariants and Dirac matrices,

$$\hat{\Gamma}_N = a \cdot I + b \cdot \gamma_\mu \times (\text{vectors})^\mu + c\gamma_5 + d \cdot \gamma_5\gamma_\mu \times (\text{vectors})^\mu,$$

to be sandwiched between final and initial nucleon spinors,

$$g_N = \bar{u}(p'_2)\hat{\Gamma}_N\left(p_2, q; \frac{p_1}{s}\right)u(p_2).$$

As we have already learned,  $\hat{\Gamma}$  depends on the momentum in the ‘alien’ vertex through the four-vector  $\hat{p}_1/s$ . Convoluting  $\gamma_\mu$  with vectors  $p_2$  and  $q$  produce  $\hat{p}_2$  and  $\hat{p}'_2$  which reduce to the scalar  $m_N$  when acting on the neighbouring spinors. So the most general expression for  $\hat{\Gamma}$  we are left with reads

$$\hat{\Gamma} = a(q^2) + b(q^2)\frac{\hat{p}_1}{s} + c(q^2)\gamma_5 + d(q^2)\gamma_5\frac{\hat{p}_1}{s}. \tag{8.59}$$

Contrary to the  $\pi\pi$  vertex, the nucleon one contains, generally speaking, four independent scalar functions. We need to understand whether all these structures are really independent or some of them can mix with each other. To this end we have to look at the  $\bar{N}N$  system in the



$t$ -channel to see what this system can transfer to; in other words, what are the quantum numbers of each of the four terms in (8.59).

Given the total angular momentum  $j$ , we have four possible states:

$$\begin{aligned} (1, 2) : \quad & \sigma = 1, \quad \ell = j \pm 1, \\ (3) : \quad & \sigma = 1, \quad \ell = j, \\ (4) : \quad & \sigma = 0, \quad \ell = j. \end{aligned} \tag{8.60}$$

Here  $\ell$  is the orbital momentum of the  $\bar{N}N$  pair and  $\sigma$  its full spin.

Bearing in mind that the *internal parity* of a fermion and its antifermion is opposite, spatial parity of the  $\bar{N}N$  pair is

$$P = (-1) \times (-1)^\ell = \begin{cases} (-1)^j & \text{for } \ell = j \pm 1, \\ (-1)^{j+1} & \text{for } \ell = j. \end{cases}$$

This separates the first two and the last two states in (8.60):

$$P_r(1, 2) = +1, \quad P_r(3, 4) = -1.$$

Consider now the charge parity  $C$  (or  $G$ -parity which generalizes it onto full isotopic multiplets). Under charge conjugation of a neutral system, say,  $p\bar{p}$ , the particle becomes an antiparticle and vice versa,

$$p(x_1, \sigma_1) + \bar{p}(x_2, \sigma_2) \rightarrow \bar{p}(x_1, \sigma_1) + p(x_2, \sigma_2).$$

To get back to the initial state one has to exchange space coordinates and spin variables. This operation results in the phase factor

$$C = (-1)^\ell \times (-1)^\sigma = \begin{cases} (-1)^j & \implies C_r = +1 & \text{for } (1, 2) \text{ and } (4), \\ (-1)^{j+1} & \implies C_r = -1 & \text{for } (3). \end{cases}$$

Now we know quantum numbers of the four states listed in (8.60):

$$\begin{aligned} (1, 2) : \quad & \sigma = 1, \quad \ell = j \pm 1, \quad P_r = +1, \quad C_r = +1, \\ (3) : \quad & \sigma = 1, \quad \ell = j, \quad P_r = -1, \quad C_r = -1, \\ (4) : \quad & \sigma = 0, \quad \ell = j, \quad P_r = -1, \quad C_r = +1. \end{aligned} \tag{8.61}$$

We conclude that the first two states can actually mix, so that we can expect three (rather than four) distinct sets of reggeons that couple to a nucleon.

It is interesting to notice that the list (8.61) does not contain one combination, namely  $(P_r, C_r) = (+, -)$ : such a state cannot be constructed from a fermion and an antifermion. Remarkably, particles with this specific combination of quantum numbers were not observed experimentally! This *may mean* that all mesons are indeed built of a fermion–antifermion pair (as in the quark model).

Let us learn how to establish spatial and charge parities for each term of the reggeon vertex (8.59). To do that we have to go into the  $t$ -channel

cms and perform the symmetry operation in one vertex (obviously, under the reflection of *both* vertices the amplitude stays invariant). We start with spatial reflection, that is, changing signs of three-momenta without touching spins. Under this operation,

$$p_2^{(t)} \rightarrow (p_{20}^{(t)}; -\mathbf{p}_2^{(t)}), \quad p_2^{\prime(t)} \rightarrow (p_{20}^{\prime(t)}; -\mathbf{p}_2^{\prime(t)}),$$

the spinors transform as follows,  $u \rightarrow \gamma_0 u$ ,  $\bar{u} \rightarrow \bar{u} \gamma_0$ , so that the vertex gets wrapped by  $\gamma_0$  matrices,

$$\hat{\Gamma}_N \rightarrow \gamma_0 \hat{\Gamma}_N \gamma_0 \quad (\gamma_0^2 = \gamma_0, \quad \gamma_0 \gamma_i \gamma_0 = -\gamma_i, \quad \gamma_0 \gamma_5 \gamma_0 = -\gamma_5).$$

Then we have to recall that  $p_1 \simeq p^+$  represents in the  $t$ -channel a circular polarization vector which has no energy component,  $p_1^{(t)} \simeq (0, \mathbf{p}_1^{(t)})$ ; as a result,  $\gamma_0 \hat{p}_1^{(t)} \gamma_0 = -\hat{p}_1^{(t)}$ . Finally, under the reflection, the  $t$ -channel scattering angle undergoes  $\Theta^{(t)} \rightarrow \Theta^{(t)} + \pi$ , so that the sign of  $s$  also has to be changed since  $s \propto \cos \Theta^{(t)}$ . All this said, we obtain

$$(a): 1 \rightarrow 1, \quad (b): \frac{\hat{p}_1}{s} \rightarrow \frac{-\hat{p}_1}{-s}, \quad (c): \gamma_5 \rightarrow -\gamma_5, \quad (d): \gamma_5 \frac{\hat{p}_1}{s} \rightarrow -\gamma_5 \frac{-\hat{p}_1}{-s},$$

which gives us  $P_r$  parity of each of the four structures in the vertex (8.59):

$$\begin{aligned} g_{(1,2)} &= \bar{u} \left[ a + b \frac{\hat{p}_1}{s} \right] u \rightarrow +g_{(1,2)}, \\ g_{(3)} &= \bar{u} \left[ c \gamma_5 \right] u \rightarrow -g_{(3)}, \\ g_{(4)} &= \bar{u} \left[ d \gamma_5 \frac{\hat{p}_1}{s} \right] u \rightarrow -g_{(4)}. \end{aligned}$$

Charge conjugation is a bit more complicated. The crossing amounts to

$$s \rightarrow u \simeq -s, \tag{8.62a}$$

and transforming the nucleon wave functions as follows,

$$u \rightarrow C^{-1} \bar{v}^T, \quad \bar{u} \rightarrow v^T C, \tag{8.62b}$$

where  $v$  is a spinor describing the antiparticle (superscript  $T$  stands for transposition), and  $C$  is the charge conjugation matrix:

$$C^{-1} \gamma_\mu C = -\gamma_\mu^T, \quad C^{-1} \gamma_5 C = \gamma_5^T. \tag{8.62c}$$

Making use of the rules (8.62) it is straightforward to derive that, differently from three other vertices, the vertex  $g_4$  has an odd charge parity.

Both spatial and charge reflections include the  $s \rightarrow -s$  operation because of which the reggeon propagator  $s^\alpha \xi_\alpha$  produces an additional factor  $(-1)^\alpha \equiv (-1)^j$ . This factor is included in the definition of  $P_r$  and  $C_r$ .

Table 8.2 Reggeons coupled with nucleon  $\rightarrow$  nucleon.

vertex	$P_r$	$C_r$	$I$	$G_r$	sgn	Reggeon
$a + b \frac{\hat{p}_1}{s}$	+	+	0	+	+	$\mathbf{P}, f(\mathbf{P}')$
			0	+	-	$\omega$
			1	-	+	$A_2$
			1	-	-	$\rho$
$c \gamma_5$	-	+	0	+	+	$\eta$
			1	-	+	$\pi$
$d \gamma_5 \frac{\hat{p}_1}{s}$	-	-	0	+	-	$f_1$
			1	-	-	$a_1$

In Table 8.2 the corresponding Regge trajectories are presented.

### 8.5.3 Spin phenomena in $\pi N$ and $NN$ scattering

We start from the  $\pi N \rightarrow \pi N$  scattering process of Fig. 8.8(a). Examining Tables 8.1 and 8.2 we conclude that reggeon exchanges with  $P_r = C_r = +1$  are possible, which include reggeons with vacuum quantum numbers,  $\mathbf{P}, f(\mathbf{P}')$ , etc. as well as negative signature trajectories like  $\rho$ . All such reggeons contribute, but at  $s \rightarrow \infty$  only the rightmost one, the pomeron  $\mathbf{P}$ , survives. In this limit elastic scattering dominates, and the amplitude can be written in the following form,

$$A_{\pi p}^{\text{el}}(s, q^2) \simeq g_\pi(q^2) \bar{u}^{\lambda'}(p'_2) \left[ a(q^2) + 2mb(q^2) \frac{\hat{p}_1}{s} \right] u^\lambda(p_2) \cdot s^\alpha \xi_\alpha, \quad (8.63)$$

where the pion residue  $g_\pi$  and the nucleon vertex functions  $a, b$  are all isospin-diagonal and refer to the pomeron,  $\alpha = \alpha_{\mathbf{P}}(q^2)$ . Indices  $\lambda$  and  $\lambda'$  marking the Dirac four-spinors stand for polarizations of the incoming and the outgoing protons, correspondingly. Let us see whether there is anything new in (8.63) compared to the case of spinless particles. We observe that the amplitude still depends on spins so that even at tremendously large energies, proton polarization changes (whereas isospin does not: charge exchange reactions, like  $\pi^- p \rightarrow \pi^0 n$ , have died out).

What may happen to spin observables in principle? There are different possibilities: a polarized nucleon may flip its spin, or lose its polarization altogether; an unpolarized one may acquire non-zero polarization, etc. What happens in reality? From the reggeon expression (8.63) it follows that only one of the whole variety of spin phenomena survives in the high

energy limit, namely the nucleon spin turns. Moreover, this occurs in a rather unusual form.

What would we expect in a simple diffraction picture? If a particle in NQM scatters at small angle, we could imagine that its spin either does not change as in Fig. 8.9(a) or turns, following the change in the particle-momentum direction (if spin and momentum are firmly tied), Fig. 8.9(b). In the relativistic case, in spite of a miniscule scattering an-

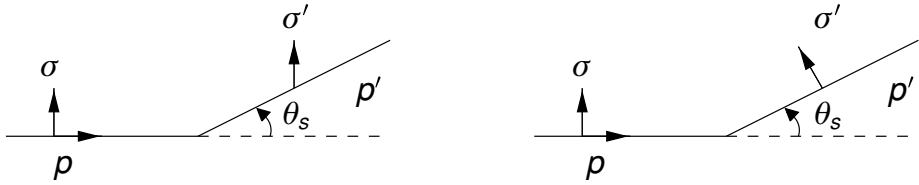


Fig. 8.9

gle  $\theta_s \simeq |\mathbf{p}'_{\perp}|/|\mathbf{p}'| \ll 1$ , the spin turns to a *large* angle,  $\theta = \mathcal{O}(1)$ , which depends on the momentum transfer but not on the collision energy. This shows that the reggeon interaction acts in a non-trivial way, independently on the momentum and the spin of the participating particle.

We start with the first term in the nucleon vertex (8.63),

$$a(q^2)\bar{u}^{\lambda'}(p'_2)u^{\lambda}(p_2),$$

and treat it in a frame where the proton is fast,  $|\mathbf{p}'_2| \simeq |\mathbf{p}_2| \gg |\mathbf{q}|$ , and scatters at a small angle

$$\theta_s \simeq \sin \theta_s; \quad \boldsymbol{\theta}_s = \frac{[\mathbf{p}_2 \times \mathbf{p}'_2]}{|\mathbf{p}_2| |\mathbf{p}'_2|} \simeq \frac{[\mathbf{e}_z \times \mathbf{q}]}{|p_{02}|}.$$

To evaluate the product of Dirac spinors we can express the final state wave function  $u(p'_2)$  via the initial state one,  $u(p'_2) = \hat{R}(\boldsymbol{\theta}_s)u(p_2)$ , using the rotation matrix  $\hat{R}$  which we expand to the first order in  $\theta_s$ :

$$\hat{R}(\boldsymbol{\theta}_s) = \begin{pmatrix} \exp(\frac{i}{2}\boldsymbol{\sigma} \cdot \boldsymbol{\theta}_s) & 0 \\ 0 & \exp(-\frac{i}{2}\boldsymbol{\sigma} \cdot \boldsymbol{\theta}_s) \end{pmatrix} \simeq \mathbf{I} + \gamma_0 \frac{i\boldsymbol{\sigma} \cdot \boldsymbol{\theta}_s}{2}.$$

This gives

$$\begin{aligned} \bar{u}^{\lambda'}(p'_2)u^{\lambda}(p_2) &\simeq \bar{u}^{\lambda'}(p_2) \left( 1 - \gamma_0 \frac{i\boldsymbol{\sigma} \cdot \boldsymbol{\theta}_s}{2} \right) u^{\lambda}(p_2) \\ &= \varphi^{\lambda'*} \left( 2m - 2p_{20} \frac{i\boldsymbol{\sigma} \cdot \boldsymbol{\theta}_s}{2} \right) \varphi^{\lambda} = \varphi^{\lambda'*} (2m + i[\boldsymbol{\sigma} \times \mathbf{q}]_z) \varphi^{\lambda}. \end{aligned}$$

Here we have represented the Dirac wave functions in terms of  $2 \times 2$  Weyl spinors  $\varphi$ ,

$$u^\lambda(p) = \begin{pmatrix} \sqrt{p_0 + m} \varphi^\lambda \\ \frac{\boldsymbol{\sigma} \cdot \mathbf{p}}{\sqrt{p_0 + m}} \varphi^\lambda \end{pmatrix},$$

and used the well known relations

$$\begin{aligned} \bar{u}^{\lambda'}(p) u^\lambda(p) &= 2m \varphi^{\lambda'*} \varphi^\lambda, \\ \bar{u}^{\lambda'}(p) \gamma_\mu u^\lambda(p) &= 2p_\mu \varphi^{\lambda'*} \varphi^\lambda. \end{aligned}$$

In the second term of the nucleon vertex we can set  $p'_2 = p_2$ , up to negligible corrections  $\mathcal{O}(s^{-1})$ , and use (8.64) to get

$$2mb \frac{p_{1\mu}}{s} \bar{u}(p'_2) \gamma^\mu u(p_2) \simeq 2mb \varphi^* \varphi \left[ \frac{p_{1\mu}}{s} \cdot 2p_2^\mu + \dots \right] \simeq 2mb(q^2) \varphi^* \varphi.$$

Combining the two terms, for the nucleon vertex we obtain the expression

$$\begin{aligned} \bar{u}^{\lambda'}(p'_2) \left[ a(q^2) + 2mb(q^2) \frac{\hat{p}_1}{s} \right] u^\lambda(p_2) \\ \simeq \varphi^{\lambda'*} (2m[a(q^2) + b(q^2)] + ia(q^2)[\boldsymbol{\sigma} \times \mathbf{q}]_z) \varphi^\lambda. \end{aligned} \tag{8.64}$$

The matrix structure of the nucleon Regge residue (8.64) tells us that the spin of the proton turns around the normal to the scattering plane,  $[\mathbf{n} \times \mathbf{n}']$ , to a finite angle  $\theta$ :

$$\tan \frac{\theta}{2} = \frac{|\mathbf{q}_\perp|}{2m} \frac{a(-\mathbf{q}_\perp^2)}{a(-\mathbf{q}_\perp^2) + b(-\mathbf{q}_\perp^2)} = \mathcal{O}(1). \tag{8.65}$$

Here a few comments are due. First of all, we see that  $\theta$  is determined by the functions  $a$  and  $b$  which describe pomeron attachment to target nucleon and do not depend on the type of the projectile. Therefore, for a given  $q$ , the nucleon spin will rotate by the same angle (8.65) in  $\pi N$  and  $NN$  scattering. Moreover, since in the single-pole approximation all spin amplitudes have the same phase (all complexity is embodied in the universal signature factor  $\xi_\alpha$ ), polarization can neither emerge nor disappear as a result of collision since these effects are proportional to an interference between amplitudes with and without ‘spin-flip’:

$$\mathcal{P} \propto \text{Im}(A_{\uparrow\uparrow}^* A_{\uparrow\downarrow}).$$

For the same reason at asymptotically high energies there is no other more subtle effects such as correlation between two spins in the  $NN$  scattering.

### 8.6 Conspiracy

Concerning  $NN$  scattering, one interesting phenomenon remains to be investigated known as ‘conspiracy’.

As we have established already, this amplitude contains three separate contributions,

$$A_{NN \rightarrow NN} = A_{(1)} \begin{pmatrix} P_r = +1 \\ C_r = +1 \end{pmatrix} + A_{(2)} \begin{pmatrix} P_r = -1 \\ C_r = +1 \end{pmatrix} + A_{(3)} \begin{pmatrix} P_r = -1 \\ C_r = -1 \end{pmatrix},$$

whose energy dependence is described by three reggeons with different, generally speaking, Regge trajectories:

$$A_{(1)} = \left( \bar{u}_1 \left[ a(q^2) + b(q^2) \frac{\hat{p}_2}{s} \right] u_1 \right) \left( \bar{u}_2 \left[ a(q^2) + b(q^2) \frac{\hat{p}_1}{s} \right] u_2 \right) s^{\alpha_1} \xi_{\alpha_1}, \tag{8.66a}$$

$$A_{(2)} = \left( \bar{u}_1 \left[ c(q^2) \gamma_5 \right] u_1 \right) \left( \bar{u}_2 \left[ c(q^2) \gamma_5 \right] u_2 \right) s^{\alpha_2} \xi_{\alpha_2}, \tag{8.66b}$$

$$A_{(3)} = \left( \bar{u}_1 \left[ d(q^2) \gamma_5 \frac{\hat{p}_2}{s} \right] u_1 \right) \left( \bar{u}_2 \left[ d(q^2) \gamma_5 \frac{\hat{p}_1}{s} \right] u_2 \right) s^{\alpha_3} \xi_{\alpha_3}. \tag{8.66c}$$

Let us take a moderately large energy where all the poles are essential, add their contributions and . . . we will be surprised! Look at the value of the amplitude at  $\mathbf{q} = 0$ , i.e. at the exactly forward scattering. Then the first amplitude (8.66a) trivializes and becomes diagonal with respect to the spin,

$$\bar{u}^{\lambda'}(p_1) \left[ \frac{\hat{p}_2}{s} \right] u^\lambda(p_1) = \frac{p_2^\mu}{s} \cdot \bar{u} \gamma_\mu u = \frac{p_2^\mu}{s} \cdot 2p_{1\mu} \cdot \delta_{\lambda\lambda'} = \delta_{\lambda\lambda'}.$$

As for the rest,  $A_{(2)}$  vanishes and  $A_{(3)}$  stays finite. To see this it suffices to look at one vertex in the rest frame, say,  $p_1 = (m, \mathbf{0})$ , where the four-spinor has only an upper component,

$$u^\lambda(p_1) = \begin{pmatrix} \varphi^\lambda \\ 0 \end{pmatrix},$$

and of three matrices,

$$\gamma_5 = \begin{pmatrix} 0 & 1 \\ -1 & 0 \end{pmatrix}, \quad \gamma_5 \gamma_0 = - \begin{pmatrix} 0 & 1 \\ 1 & 0 \end{pmatrix}, \quad \gamma_5 \gamma_i = - \begin{pmatrix} \sigma_i & 0 \\ 0 & \sigma_i \end{pmatrix},$$

only the last one (diagonal) survives,

$$\bar{u}(p_1) \gamma_5 \gamma u(p_1) = \varphi_1^* \boldsymbol{\sigma} \varphi_1 \equiv \boldsymbol{\sigma}^{(1)},$$

yielding the matrix element  $\sigma_z^{(1)}$  upon multiplication by  $p_{2\mu}$  in (8.66c). Thus from  $A_{(1)}$  and  $A_{(3)}$  we have two contributions to the forward

amplitude:

$$A(q = 0) = c + c'\sigma_z^{(1)}\sigma_z^{(2)}; \tag{8.67}$$

$\mathbf{z}$  is the collision axis as before.

This expression is formally legitimate (the  $\mathbf{z}$ -direction is special, while rotational symmetry in the transverse plane is respected). Still it looks strange: from general considerations we could expect the presence of another term in (8.67)

$$\dots + c''(\boldsymbol{\sigma}_\perp^{(1)} \cdot \boldsymbol{\sigma}_\perp^{(2)}) = c''(\sigma_x^{(1)}\sigma_x^{(2)} + \sigma_y^{(1)}\sigma_y^{(2)}). \tag{8.68}$$

Why have we lost this invariant? It is not a question of the asymptotic behaviour since we have added all Regge pole contributions; so, what has happened?

Let us see whether we could restore the term (8.68) in the forward scattering amplitude. We have to be a bit more accurate. Taking the  $q = 0$  limit in (8.66a), we have dropped the second, linear in  $\mathbf{q}$ , term in the full expression (8.64) for the first amplitude,

$$\propto ia(-\mathbf{q}_\perp^2)[\boldsymbol{\sigma} \times \mathbf{q}_\perp]_z \quad \left( \propto \sigma_x \quad \text{for } \mathbf{q}_\perp \parallel \mathbf{y} \right). \tag{8.69}$$

This would have been a bad idea if the coefficient was *singular* at  $q_\perp = 0$ . Imagine that we force this contribution to be *finite* in the  $q_\perp \rightarrow 0$  limit. The result is bizarre: the amplitude would remember about the direction of the vector  $\mathbf{q}_\perp$  before it vanished! Indeed, if  $\mathbf{q}$  is directed along the  $\mathbf{y}$ -axis, the rescued term contains the matrix  $\sigma_x$ , as envisaged in (8.69). So, we have found the  $\sigma_x \otimes \sigma_x$  term rather than the full  $\sigma_\perp \otimes \sigma_\perp$  of (8.68).

Let us search for the missing  $\sigma_y \otimes \sigma_y$ . The vertex in  $A_{(2)}$  is a *pseudoscalar* and should therefore contain  $\varphi^*(\boldsymbol{\sigma} \cdot \mathbf{q}_\perp)\varphi \propto \sigma_y$  (and the coefficient  $c(q^2)$  in (8.66b) could also be singular). Indeed, rewriting (8.66) in the two-component form at small momentum transfer, we obtain

$$A_{(1)} = \left\{ f_1 + f_2[\boldsymbol{\sigma}^{(1)} \times \mathbf{q}_\perp]_z \right\} \left\{ f_1 + f_2[\boldsymbol{\sigma}^{(2)} \times \mathbf{q}_\perp]_z \right\} s^{\alpha_1} \xi_{\alpha_1}, \tag{8.70a}$$

$$A_{(2)} = f_3^2 \left( \boldsymbol{\sigma}^{(1)} \cdot \mathbf{q}_\perp \right) \left( \boldsymbol{\sigma}^{(2)} \cdot \mathbf{q}_\perp \right) s^{\alpha_2} \xi_{\alpha_2}, \tag{8.70b}$$

$$A_{(3)} = f_4^2 \sigma_z^{(1)} \sigma_z^{(2)} s^{\alpha_3} \xi_{\alpha_3}, \tag{8.70c}$$

where  $f_i = f_i(q^2)$  and  $\boldsymbol{\sigma}^{(i)} \equiv \varphi_i^* \boldsymbol{\sigma} \varphi_i$ .

The strategy of restoring the lost contribution (8.68) is now clear:  $f_2$  and  $f_3$  must be both singular and, moreover, have to have the same  $q \rightarrow 0$

limit,

$$f_2^2(q_\perp^2) \simeq f_3^2(q_\perp^2) \simeq \frac{c''}{\mathbf{q}_\perp^2} \quad \text{at } \mathbf{q}_\perp \rightarrow 0. \quad (8.71a)$$

But the two pieces,  $\sigma_x\sigma_x$  and  $\sigma_y\sigma_y$ , belong to different trajectories! In order to preserve the rotational invariance in the  $\{x, y\}$  plane at *all energies*, the vacuum trajectory ( $A_{(1)}$ ) must *cross* with a trajectory with  $\pi$ -meson quantum numbers ( $A_{(2)}$ ) at  $t = 0$ . This explains the name *conspiracy*: two reggeons must ‘make a deal’ concerning both their trajectories and residues,

$$\alpha_1(0) = \alpha_2(0), \quad r_1(0) = r_2(0). \quad (8.71b)$$

Is this a miracle? Not entirely. We have lost, in the first place, (8.68) because  $(\boldsymbol{\sigma}_\perp \cdot \boldsymbol{\sigma}_\perp)$  does not correspond to a state with definite quantum numbers in the  $t$ -channel: it has a mixture of two states with different *parity*.

Recall what was the reason for Regge trajectories with differing quantum numbers to be different? It was the *unitarity* that separated them. Satisfying different unitarity conditions, two reggeons have no reason to be related *unless* there is a specific symmetry in the works. Is there not an additional symmetry at  $t = 0$ ? Obviously, there is.

What is the *parity* of a given object? We go to its rest frame and see which sign the wave function acquires under the spatial reflection. However, if a particle has  $m = 0$ , one cannot stop it and the notion of parity loses sense. But the point  $t = 0$  corresponds exactly to a zero mass object in the  $t$ -channel, and our states  $A_{(1)}$  and  $A_{(2)}$ , which differed only by their parity,  $P_r = \pm$ , become physically indistinguishable. Certainly, this argument does not *prove* the conspiracy phenomenon but makes its possible existence less mysterious.

From the point of view of the interaction in the  $t$ -channel, the conspiracy means that the ‘potential’ possesses an additional symmetry at  $t = 0$  which prevents the unitarity condition from separating the amplitudes with different parities. A closer examination of various reactions shows that the conditions (8.71) are not sufficient. Having made  $f_i$  singular, we did something serious: inserted a singularity that the total amplitude should not have. As a remedy, another Regge trajectory must enter the conspiracy plot, with an intercept smaller by one unity. (Actually, a whole series of shifted trajectories – ‘daughters’ – appear.)

To conclude, if forward-scattering amplitudes contain the contribution proportional to  $(\boldsymbol{\sigma}_\perp \cdot \boldsymbol{\sigma}_\perp)$  then, within the Regge-pole approach, this is an evidence for conspiracy. Experimentally such a phenomenon is not



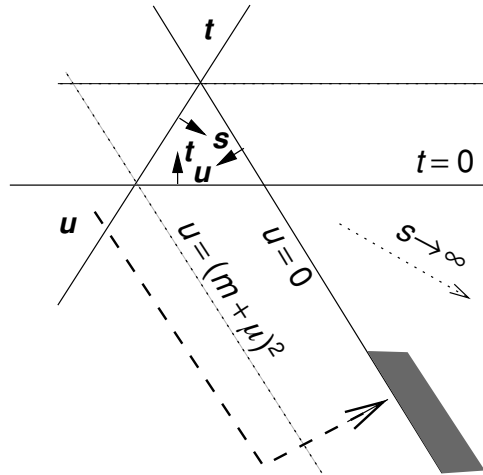


Fig. 8.10 Backward  $\pi N$  scattering on the Mandelstam plane.

observed so far. In any case, an experimental proof is difficult because of the influence of the *reggeon branchings*.

### 8.7 Fermion Regge poles

Up to now we have studied the behaviour of two-particle scattering amplitudes in the region  $|t| \sim m^2$ ,  $s \rightarrow \infty$ . However, since we formally allowed an incident particle to change identity, this means that we have already treated the backward scattering as well! Look, for example, at the region  $|u| \sim m^2$ ,  $s \rightarrow \infty$  in the  $\pi N \rightarrow \pi N$  scattering amplitude shown on the Mandelstam plane in Fig. 8.10.

What is so remarkable about this region? In Lecture 5 we have seen that in the relativistic theory there exists, in addition to a forward peak, also one in the backward direction. The magnitude of the backward peak depends on how willingly the particle is ready to change its individuality (recall the Compton effect).

With the help of the theory of complex angular momenta we have learned how to write the asymptotics for the scattering of spinless particles at a small angle  $\theta_s = \sqrt{-t/s}$  and found that it was determined by quantum numbers in the  $t$ -channel. Later, we have generalized the obtained results to the case of non-zero spin particles.

Obviously, the same programme can be carried out also for backward scattering,  $\theta_u = \sqrt{-u/s} \ll 1$ . In the case of spinless particles, or particles with integer spins, the whole story will be a mere repetition, the

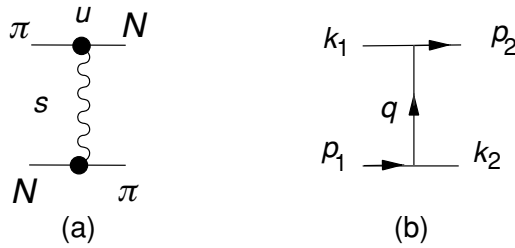


Fig. 8.11 (a) Backward  $\pi N$  scattering; (b)  $u$ -channel fermion exchange.

only difference being that the asymptotics will now be determined by the quantum numbers of the  $u$ -channel exchange. In a backward scattering of a fermion, e.g. backward  $\pi N$  scattering shown in Fig. 8.11(a), an interesting new phenomenon appears owing to the fact that the exchange is now carried out by a reggeon with a *half-integer* angular momentum. Let us investigate this case in detail.

How to write an amplitude corresponding to a fermion exchange? Let us turn to the perturbation theory. The exchange amplitude for a particle with  $\sigma = \frac{1}{2}$  shown in Fig. 8.11(b) has the form

$$A(s, u) = \bar{u}(p_2)g(q^2)\frac{1}{m - \hat{q}}g(q^2)u(p_1), \quad q = p_1 - k_2. \tag{8.72}$$

Given the spinor normalization  $u(p) \sim \sqrt{p_0}$ , at large  $s$  this amplitude behaves as  $A[\sigma = \frac{1}{2}] \propto \sqrt{s} = s^\sigma$ , as expected.

If we have a  $\sigma = \frac{3}{2}$  particle exchange, the longitudinal polarization tensor,  $e_\mu^- e_\nu^+ \propto p_{1\mu}k_{1\nu}/s$ , convolutes with the momenta in the vertices,  $k_1^\mu p_1^\nu$  and produces an extra  $s$ , yielding  $A[\sigma = \frac{3}{2}] \sim s^\sigma$ , etc.

Generalizing to the case of an arbitrary spin as before, we shall write the reggeon exchange amplitude as (cf. (8.63))

$$A(s, u) = \bar{u}(p_2)[a(q^2) + b(q^2)\hat{q}]u(p_1)s^{\alpha(q^2) - \frac{1}{2}}\xi_{\alpha(q^2) - \frac{1}{2}}. \tag{8.73}$$

Here we put  $\alpha - \frac{1}{2}$  in the exponent since spinors provide an additional factor  $\sqrt{s}$ , as they already did before in (8.72).

Following our logic, let us determine the quantum numbers in the  $u$  channel. If we assume that there is no degeneracy so that unitarity does separate trajectories with different quantum numbers, we need to learn to write amplitudes with definite parity which correspond to two opposite parity  $u$ -channel states with  $\ell = j \pm \frac{1}{2}$ .

To do so, we move, as usual, to the  $u$ -channel cms and carry out spatial reflection in one of the vertices, e.g. in the lower one in Fig. 8.11b. The

matrix  $\hat{q}$ , transversal in the  $s$  channel, in the  $u$ -channel centre-of-mass frame has only a time component:

$$\hat{q}_{(u)} = \gamma_0 q_{0(u)} = \gamma_0 \sqrt{q^2}.$$

The spinor  $u(p_1)$  under reflection produces

$$u(\mathbf{p}_1) \implies i\gamma_0 u(\mathbf{p}_1).$$

Then, the cosine of the  $u$ -channel scattering angle changes sign,  $z_u = \cos \theta_u \rightarrow -z_u$ , which corresponds to the reflection  $s \rightarrow -s$ , yielding the factor  $(-1)^{\alpha - \frac{1}{2}}$ . Altogether, the parity operation acts on the amplitude as follows:

$$A \propto [a + bq_{0(u)} \cdot \gamma_0] \implies [a \cdot \gamma_0 + bq_{0(u)}](-1)^\alpha.$$

To have a definite parity  $P_r = P \cdot (-1)^\alpha$ , one of the conditions

$$a\gamma_0 + bq_{0(u)} = \pm(a + bq_{0(u)}\gamma_0)$$

has to be satisfied, that is, returning to the Lorentz invariant form,

$$a(q^2) = \pm b(q^2)\sqrt{q^2}.$$

Thus, the contribution of a fermionic Regge pole with a definite parity  $P_r$  reads

$$A_\pm = r^\pm (q^2) \bar{u}(p_2) [\hat{q} \pm \sqrt{q^2}] u(p_1) \cdot s^{\alpha_\pm - 1/2} \xi_{\alpha_\pm - 1/2}. \quad (8.74)$$

We see right away that  $A_\pm(s, u)$  have rather unusual features.

- (1) The existence of a singularity at  $q^2=0$  contradicts the analytic structure of the Mandelstam plane where the first  $u$ -channel (threshold) singularity appears at  $q^2 = u = (m + \mu)^2 > 0$ .
- (2) In the physical region of the  $s$ -channel ( $q^2 \leq 0$ ) the complexity of  $A_\pm$  is not limited to the complexity of the signature factor.

Hence, we cannot assume that the high-energy behaviour of the backward scattering is determined by a single pole of definite parity without contradicting analyticity of the scattering amplitude in  $u$ . The only way to avoid this contradiction is to say that the asymptotics is determined by both poles simultaneously:

$$\begin{aligned} A = A_+ + A_- &= r^+ \bar{u}_2(\hat{q} + \sqrt{q^2}) u_1 s^{\alpha_+ - \frac{1}{2}} \xi_{\alpha_+ - \frac{1}{2}} \\ &\quad + r^- \bar{u}_2(\hat{q} - \sqrt{q^2}) u_1 s^{\alpha_- - \frac{1}{2}} \xi_{\alpha_- - \frac{1}{2}}, \end{aligned} \quad (8.75a)$$

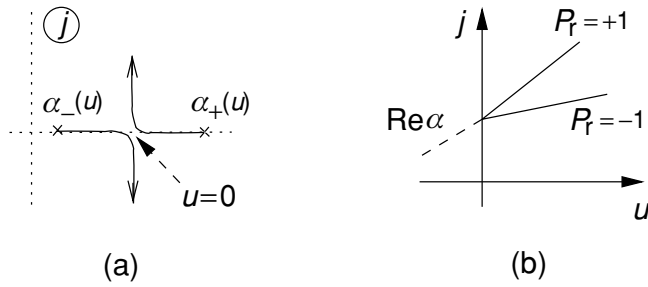


Fig. 8.12 (a) Movement of fermionic reggeons from positive to negative  $u$  on the  $j$  plane; (b) conspiracy of fermionic trajectories on the Chew–Frautschi plot.

where the two trajectories derive from one function, as do the residues:

$$\alpha^+ \equiv \alpha(\sqrt{u}), \quad \alpha^- = \alpha(-\sqrt{u}); \quad (8.75b)$$

$$r^+ \equiv r(\sqrt{u}), \quad r^- = r(-\sqrt{u}). \quad (8.75c)$$

Let us see what are the consequences of this picture.

*Conspiracy.* First of all, how do the Regge trajectories  $\alpha^\pm(u)$  behave?

$u > 0$ : the physical region of the  $u$ -channel. The trajectories  $\alpha_+$  and  $\alpha_-$  are values of the same function of different real arguments.

$u < 0$ : the physical region of the  $s$ -channel; the arguments are imaginary, complex conjugate, and we have

$$\alpha_+ = \alpha(i\sqrt{-u}) = \alpha^*(-i\sqrt{-u}) = \alpha_-^*.$$

The possible behaviour of the poles in the  $j$ -plane while moving from one region to the other is shown in Fig. 8.12(a). At  $u > 0$  the trajectories are real and, generally speaking, different, see Fig. 8.12(b). They cross at  $u = 0$  ('conspiracy'); at  $u < 0$  they become complex conjugate and diverge in the  $j$  plane.

So our attempt to separate fermionic trajectories with different parities, without violating the analyticity, has led us to unavoidable conspiracy. As we have already discussed above in Section 8.6, this phenomenon is due to the uncertainty in the parity of a massless particle.

Let us demonstrate this in perturbation theory. Suppose that an exchange with a Fermi-particle  $\nu$  takes place described by the diagram in

Fig. 8.11(b) (one can imagine, e.g., backward  $\pi^- e^-$  scattering via neutrino exchange). If  $m_\nu \neq 0$ , we can write two different amplitudes:

$$\begin{aligned} A_1 &= \bar{u}_2 \cdot (i\gamma_5) \frac{m_\nu + \hat{q}}{m_\nu^2 - q^2} \cdot (i\gamma_5) u_1 = \bar{u}_2 \frac{m_\nu - \hat{q}}{m_\nu^2 - q^2} u_1, \\ A_2 &= \bar{u}_2 \cdot \frac{m_\nu + \hat{q}}{m_\nu^2 - q^2} \cdot u_1. \end{aligned}$$

On the mass shell,  $q^2 = m_\nu^2$ , the parity of the amplitude  $A_1$  is  $P_1 = -i$  (here we, again, have to carry out a reflection in one of the vertices in the cms of the  $u$ -channel); the parity of the second amplitude ( $A_2$ ) is  $P_2 = i$ . Taking now  $m_\nu = 0$ , the two amplitudes become indistinguishable,

$$A_1 = \bar{u}_2 \frac{\hat{q}}{q^2} u_1 = -A_2,$$

and we arrive at a degeneracy in parity.

*Oscillations.* Since the backward scattering amplitude is described by a pair of *complex conjugate* fermionic Regge poles, this should lead to oscillations, both in  $s$  and  $u$ . Parameterizing  $\alpha_\pm(u) = \alpha_1(u) \pm i\alpha_2(u)$ , the amplitude can be represented as follows:

$$\begin{aligned} A(s, u) &= |r(u)| s^{\alpha_1 - \frac{1}{2}} \cdot \bar{u}(p_2) \left[ f_1 \hat{\mathbf{q}}_\perp + f_2 \sqrt{\mathbf{q}_\perp^2} \right] u(p_1); \\ f_1 &= f \cos[\alpha_2(u) \ln s + \varphi(u)], \quad f_2 = f \sin[\alpha_2(u) \ln s + \varphi(u)]. \end{aligned} \tag{8.76}$$

To observe these oscillations turns out to be not so simple. Indeed, if we consider the cross section

$$\frac{d\sigma}{d\Omega} \propto \frac{1}{s} AA^\dagger$$

summed (averaged) over the polarization of the final (initial) nucleon,

$$\frac{d\sigma}{d\Omega} \propto \frac{1}{2} \text{Tr}(A \cdot (\hat{p}_1 + m) \cdot \bar{A} \cdot (\hat{p}_2 + m)), \quad \bar{A} = \gamma_0 A \gamma_0,$$

the oscillations will not manifest themselves, since here the sum  $|f_1|^2 + |f_2|^2$  enters, and we obtain

$$\frac{d\sigma}{d\Omega} \propto |r(u)|^2 s^{2(\alpha_1(u)-1)} \cdot f^2(u).$$

The cross section will not oscillate even if we measure the polarization of *one* of the nucleons; only the *spin correlation* between the initial and final fermions will be an oscillating function of energy.

Thus, the theory, in the pole approximation, predicts that:

- (1) the baryon resonances lie on Regge trajectories;
- (2) cross sections with baryon number exchange decrease as powers of  $s$ ;
- (3) trajectories with different parities conspire at  $u = 0$ ; and
- (4) in the asymptotics of the amplitude there are unusual oscillations.

Indeed, many fermionic resonances, up to very high spins, are observed experimentally. Surprisingly, their trajectories look linear in the mass squared,  $u = m^2$ , similarly to the bosonic case (see Fig. 8.1 on page 180), in spite of the fact that the fermion propagator depends on the first power of the mass,  $G \propto 1/(m - \hat{q})$ , rather than on  $m^2$  as boson propagators do. This means that in the series expansion for the analytic function  $\alpha$  which determines the nucleon trajectories according to (8.75b), the square-root term is very small, if not altogether absent:

$$\alpha(\sqrt{u}) \simeq \alpha_0 + \alpha_1\sqrt{u} + \alpha_2u + \dots, \quad \alpha_1 \simeq 0.$$

But if this is the case then according to (8.75b) there must be *parity degeneracy* for all values of  $u$ :  $\alpha^+(u) = \alpha^-(u) \simeq \alpha_0 + \alpha_2u$ . Hence, there must exist resonances with opposite parity and *equal masses*, lying on the same trajectory. This is, however, not observed experimentally.

In order to reconcile the theory with the experiment, one can try to ‘conceal’ this degeneracy by putting the residue of one of the two trajectories equal zero in the position of an unwanted resonance. This may look weird (indeed, how to force a resonance not to interact with anything in the theory of strong interactions?), but in some *dual models* (see Lecture 16) such a possibility is considered.

So, at the moment we have the following situation. On the one hand, we do see fermionic Regge poles. On the other hand, there must be an additional trick in Nature that makes the apparent linearity of baryon trajectories and the absence of parity degeneracy in the spectrum of baryon resonances consistent.